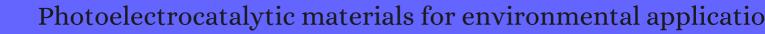
# CITATION REPORT List of articles citing



DOI: 10.1039/b821991e Journal of Materials Chemistry, 2009, 19, 5089.

Source: https://exaly.com/paper-pdf/47071743/citation-report.pdf

Version: 2024-04-09

This report has been generated based on the citations recorded by exaly.com for the above article. For the latest version of this publication list, visit the link given above.

The third column is the impact factor (IF) of the journal, and the fourth column is the number of citations of the article.

#	Paper	IF	Citations
840	A Brief Survey of the Potential Health Risks of TiO2 Particles and TiO2- Containing Photocatalytic or Non-Photocatalytic Materials. <b>2010</b> , 13,		5
839	Preparation of Bismuth Oxide Quantum Dots and their Photocatalytic Activity in a Homogeneous System. <b>2010</b> , 2, 1115-1121		29
838	Porous photocatalysts for advanced water purifications. <i>Journal of Materials Chemistry</i> , <b>2010</b> , 20, 4512		289
837	Heterointegration of Pt/Si/Ag Nanowire Photodiodes and Their Photocatalytic Properties. <b>2010</b> , 20, 3005-3011		27
836	Halbleitergassensoren: Trockensynthese und Anwendung. <i>Angewandte Chemie</i> , <b>2010</b> , 122, 7796-7825	3.6	7
835	Semiconductor gas sensors: dry synthesis and application. <i>Angewandte Chemie - International Edition</i> , <b>2010</b> , 49, 7632-59	16.4	404
834	Citric acid assisted solvothermal synthesis of BiFeO3 microspheres with high visible-light photocatalytic activity. <b>2010</b> , 331, 15-20		138
833	Nonaqueous seeded growth of flower-like mixed-phase titania nanostructures for photocatalytic applications. <b>2010</b> , 183, 1917-1924		28
832	Novel (and better?) titania-based photocatalysts: Brookite nanorods and mesoporous structures. <b>2010</b> , 216, 183-193		68
831	Visible-light sensitive cobalt-doped BiVO4 (Co-BiVO4) photocatalytic composites for the degradation of methylene blue dye in dilute aqueous solutions. <b>2010</b> , 99, 214-221		227
830	Some views about indoor air photocatalytic treatment using TiO2: Conceptualization of humidity effects, active oxygen species, problem of C1\$\mathbb{U}\$3 carbonyl pollutants. <b>2010</b> , 99, 428-434		98
829	Photocatalytical Properties of TiO2 Nanotubes. <b>2010</b> , 162, 295-328		27
828	New Photocatalyst Electrodes and Their Photocatalytic Degradation Properties of Organics. <b>2010</b> , 14, 709-727		4
827	Direct Synthesis of Photocatalytically Active Rutile TiO2 Nanorods Partly Decorated with Anatase Nanoparticles. <b>2010</b> , 114, 4909-4915		88
826	Visible Light Induced Photocatalytic Degradation of Rhodamine B on One-Dimensional Iron Oxide Particles <b>2010</b> , 114, 17051-17061		196
825	Thermal chemistry and photochemistry of hexafluoroacetone on rutile TiO2(110). <b>2010</b> , 12, 8084-91		16
824	Photocatalytic Properties of Porous Silicon Nanowires. <i>Journal of Materials Chemistry</i> , <b>2010</b> , 20, 3590-3	594	112

# (2011-2010)

823	Novel NE-Codoped TiO2 Inverse Opal with a Hierarchical Meso-/Macroporous Structure: Synthesis, Characterization, and Photocatalysis. <b>2010</b> , 114, 15251-15259	74
822	Tailored Titanium Dioxide Nanomaterials: Anatase Nanoparticles and Brookite Nanorods as Highly Active Photocatalysts. <b>2010</b> , 22, 2050-2060	347
821	Anisotropic growth of multi-twinned goethite particles by oriented aggregation. 2010, 12, 4007	7
820	Rational design and synthesis of freestanding photoelectric nanodevices as highly efficient photocatalysts. <b>2010</b> , 10, 1941-9	59
819	Visible-light-driven surface reconstruction of mesoporous TiO2: toward visible-light absorption and enhanced photocatalytic activities. <b>2011</b> , 47, 8584-6	30
818	The relationship between photocatalytic activity and photochromic state of nanoparticulate silver surface loaded titanium dioxide thin-films. <b>2011</b> , 13, 13827-38	35
817	Nickel(II) oxide surface-modified titanium(IV) dioxide as a visible-light-active photocatalyst. <b>2011</b> , 47, 8814-6	52
816	Molecular Structures, Acid <b>B</b> ase Properties, and Formation of Group 6 Transition Metal Hydroxides. <b>2011</b> , 115, 8072-8103	50
815	Solid-solid interface formation in TiO2 nanoparticle networks. <b>2011</b> , 27, 1946-53	45
814	Structural and Electronic Near Degeneracy of M3O9[[M = Cr, Mo, W). <b>2011</b> , 115, 19190-19196	27
813	Aerosol-spraying preparation of a mesoporous hollow spherical BiFeO3 visible photocatalyst with enhanced activity and durability. <b>2011</b> , 47, 2089-91	87
812	Nanostructured Materials for Photolytic Hydrogen Production. <b>2011</b> , 441-486	3
811	Enhanced Photocatalytic and Photoelectrochemical Activity in the Ternary Hybrid of CdS/TiO2/WO3 through the Cascadal Electron Transfer. <b>2011</b> , 115, 9797-9805	221
810	Tuning of the Crystallite and Particle Sizes of ZnO Nanocrystalline Materials in Solvothermal Synthesis and Their Photocatalytic Activity for Dye Degradation. <b>2011</b> , 115, 13844-13850	206
809	Controllable synthesis of mesoporous FIIiO2 spheres for effective photocatalysis. <i>Journal of Materials Chemistry</i> , <b>2011</b> , 21, 11430	111
808	Ligand-mediated shape control in the solvothermal synthesis of titanium dioxide nanospheres, nanorods and nanowires. <b>2011</b> , 3, 3799-804	14
807	Hierarchical N-doped TiO2 hollow microspheres consisting of nanothorns with exposed anatase {101} facets. <b>2011</b> , 47, 6942-4	104
806	A kinetic study of ozone decomposition on illuminated oxide surfaces. <b>2011</b> , 115, 11979-87	47

805	Highly active and enhanced photocatalytic silicon nanowire arrays. 2011, 3, 3269-76	85
804	Photodeposition of metal sulfide quantum dots on titanium(IV) dioxide and the applications to solar energy conversion. <b>2011</b> , 40, 4232-43	198
803	Fe2O3/carbon quantum dots complex photocatalysts and their enhanced photocatalytic activity under visible light. <b>2011</b> , 40, 10822-5	266
802	Effect of nitrogen and intrinsic defect complexes on conversion efficiency of ZnO for hydrogen generation from water. <b>2011</b> , 13, 15973-6	22
801	Multifunctional iron-carbon nanocomposites through an aerosol-based process for the in situ remediation of chlorinated hydrocarbons. <b>2011</b> , 45, 1949-54	70
800	New Insights into the Mechanism of TiO2 Photocatalysis: Thermal Processes beyond the Electron⊞ole Creation. <b>2011</b> , 115, 19676-19685	40
799	Enhancing photocatalytic activity of titania materials by using porous structures and the addition of gold nanoparticles. <i>Journal of Materials Chemistry</i> , <b>2011</b> , 21, 20-28	117
798	Enhancing photocatalytic activity of one-dimensional KNbO3 nanowires by Au nanoparticles under ultraviolet and visible-light. <b>2011</b> , 3, 5161	114
797	Visible-Light-Active Iron Oxide-Modified Anatase Titanium(IV) Dioxide. <b>2011</b> , 115, 6478-6483	86
796	Crystal facet engineering of semiconductor photocatalysts: motivations, advances and unique properties. <b>2011</b> , 47, 6763-83	753
795	In-situ MIR-IR Observation of Peroxo Species on Anatase TiO2 Particle during Oxygen Photoevolution Reaction. <b>2011</b> , 79, 787-789	6
794	Quasi-Aligned AgNb2O5 Nanobelt Arrays with Enhanced Photocatalytic and Antibacterial Activities. <b>2011</b> , 94, 2330-2338	32
793	Microstructures and photocatalytic properties of Ag+ and La3+ surface codoped TiO2 films prepared by solgel method. <b>2011</b> , 184, 2770-2775	38
792	Synthesis and enhanced photocatalytic activity of tin oxide nanoparticles coated on multi-walled carbon nanotube. <b>2011</b> , 46, 1372-1376	47
791	Y4Al2O9 hierarchically nanostructured microspheres assembled with nanosheets: Microwave-solvothermal synthesis combined with thermal treatment and photocatalytic property. <b>2011</b> , 65, 2793-2796	9
790	Visible light photocatalytic activity enhancement for water purification in Cu(II)-grafted WO3 thin films grown by photoreaction of nanoparticles. <b>2011</b> , 108-109, 47-53	28
789	Photoresponse and stability improvement of ZnO nanorod array thin film as a single layer of photoelectrode for photoelectrochemical water splitting. <b>2011</b> , 36, 15538-15547	61
788	Applied low bias with high frequency for enhancing mineralization ability of WO3 as visible-light-driven photocatalyst in gas phase. <b>2011</b> , 16, 180-183	10

# (2011-2011)

787	Photocatalysis in TiO2 aqueous suspension: Effects of mono- or di-hydroxyl substitution of butanedioic acid on the disappearance and mineralisation rates. <b>2011</b> , 178, 51-57		15
786	Mechanisms in Heterogeneous Photocatalysis. <b>2011</b> , 1-5		3
7 <sup>8</sup> 5	Stability of nanocomposites of poly(Eaprolactone) with tungsten trioxide. 2011, 18, 1743-1749		13
7 <sup>8</sup> 4	Assembly, characterization, and photocatalytic activities of TiO2 nanotubes/CdS quantum dots nanocomposites. <b>2011</b> , 13, 6661-6672		30
783	Layered Fe(III) doped TiO2 thin-film electrodes for the photoelectrocatalytic oxidation of glucose and potassium hydrogen phthalate. <b>2011</b> , 56, 2475-2480		3
782	Nanostructured Tungsten Oxide iProperties, Synthesis, and Applications. <b>2011</b> , 21, 2175-2196		994
781	Titanium(IV) Dioxide Surface-Modified with Iron Oxide as a Visible Light Photocatalyst. <i>Angewandte Chemie</i> , <b>2011</b> , 123, 3563-3567	3.6	33
7 <sup>8</sup> 0	Titanium(IV) dioxide surface-modified with iron oxide as a visible light photocatalyst. <i>Angewandte Chemie - International Edition</i> , <b>2011</b> , 50, 3501-5	16.4	169
779	Fe3O4/WO3 hierarchical core-shell structure: high-performance and recyclable visible-light photocatalysis. <b>2011</b> , 17, 5145-54		224
778	Visible-light-induced dye degradation over copper-modified reduced graphene oxide. <b>2011</b> , 17, 2428-34		74
777	Structure analysis and photocatalytic properties of spinel zinc gallium oxonitrides. <b>2011</b> , 17, 12417-28		12
776	Electrodeposition of CdS from acidic aqueous thiosulfate solutionInvesitigation of the mechanism by electrochemical quartz microbalance technique. <b>2011</b> , 56, 5731-5739		41
775	Fabrication and photocatalytic performance of a ZnxCd1\( \text{S} \) solid solution prepared by sulfuration of a single layered double hydroxide precursor. <b>2011</b> , 102, 147-156		146
774	Hydrothermal synthesis of C-doped Zn3(OH)2V2O7 nanorods and their photocatalytic properties under visible light illumination. <b>2011</b> , 257, 3920-3923		15
773	Enhanced visible light photocatalytic activity of novel Pt/C-doped TiO2/PtCl4 three-component nanojunction system for degradation of toluene in air. <b>2011</b> , 187, 509-16		76
772	Investigation of cation (Sn2+) and anion (N3-) substitution in favor of visible light photocatalytic activity in the layered perovskite K2La2Ti3O10. <b>2011</b> , 189, 502-8		52
771	Facile synthesis and catalytic activity of MoS(2)/TiO(2) by a photodeposition-based technique and its oxidized derivative MoO(3)/TiO(2) with a unique photochromism. <b>2011</b> , 354, 607-10		97
770	Interfacial chemical bonding effect on the photocatalytic activity of TiO2-SiO2 nanocoupling systems. <b>2011</b> , 361, 628-31		27

Photodeposition of Metal Sulfide Quantum Dots on Titanium(IV) Dioxide and its Applications. **2011**, 1352, 141

-(0	(Canan) Photographytic Synthogic Employing Nitropromatic Compayade 2011 1353 110	
768	(Green) Photocatalytic Synthesis Employing Nitroaromatic Compounds. <b>2011</b> , 1352, 119	
767	Selective Photooxidation and Photoreduction Processes at Surface-Modified by Grafted Vanadyl. <b>2011</b> , 2011, 1-10	8
766	Synthesis and Photocatalytic Property of ZnO/TiO2 Inverse Opals Films with Controllable Composition and Topology. <b>2012</b> , 25, 235-241	1
765	Semiconducting transition-metal oxides based on d5 cations: Theory for MnO and Fe2O3. <b>2012</b> , 85,	66
764	ONE-STEP AND CONTROLLABLE SELF-ASSEMBLY OF Au/TiO2/CARBON SPHERES TERNARY NANOCOMPOSITES WITH A NANOPARTICLE MONOSHELL WALL. <b>2012</b> , 07, 1250025	6
763	Enhanced Visible Light Photocatalytic Activity of V2O5 Cluster Modified N-Doped TiO2 for Degradation of Toluene in Air. <b>2012</b> , 2012, 1-10	31
762	Influence of Coexisting Electron Donor Species on Charge Transfer in Dye-Sensitized Nanocrystalline TiO2 for H2 Evolution under Visible Light. <b>2012</b> , 85, 1268-1276	6
761	Superior photocatalytic activity of bimetallic Cd-Ag-ZnO for the degradation of azo dyes under UV light. <b>2012</b> , 1, 157-163	6
760	Facile Fabrication of Heterostructured Bi2O3᠒nO Photocatalyst and Its Enhanced Photocatalytic Activity. <b>2012</b> , 116, 26306-26312	220
759	Visible Photocatalytic Activity Enhancement of ZnWO4 by Graphene Hybridization. <i>ACS Catalysis</i> , <b>2012</b> , 2, 2769-2778	236
758	Review of methane mitigation technologies with application to rapid release of methane from the Arctic. <b>2012</b> , 46, 6455-69	58
757	Biogenic synthesis of photocatalytically active Ag/TiO2 and Au/TiO2 composites. <b>2012</b> , 14, 968	38
756	Nitrogen-doped titanate-anatase core-shell nanobelts with exposed {101} anatase facets and enhanced visible light photocatalytic activity. <b>2012</b> , 134, 5754-7	284
755	On the way to the creation of next generation photoactive materials. <b>2012</b> , 19, 3666-75	53
754	Aerosol flow synthesis of N, Si-codoped TiO2 hollow microspheres with enhanced visible-light driven photocatalytic performance. <b>2012</b> , 29, 189-193	15
753	Porous tungsten oxide nanoflakes for highly alcohol sensitive performance. <b>2012</b> , 4, 7078-83	28
75²	Fabrication, Characterization and Photocatalytic Capability of ZnAl2O4 Nanospheres. <b>2012</b> , 518-523, 736-739	5

# (2012-2012)

751	A simple approach to strontium sodium tantalite mesocrystals with ultra-high photocatalytic properties for water splitting. <i>Journal of Materials Chemistry</i> , <b>2012</b> , 22, 5609	37
75 <sup>0</sup>	Mesoporous TiO2 photocatalytic films on stainless steel for water decontamination. <b>2012</b> , 2, 147-155	36
749	Tin oxide-surface modified anatase titanium(IV) dioxide with enhanced UV-light photocatalytic activity. <b>2012</b> , 14, 705-11	32
748	Ag3PO4/SnO2 semiconductor nanocomposites with enhanced photocatalytic activity and stability. <b>2012</b> , 36, 1541	174
747	Toward dynamic control over TiO2 nanocrystal monolayer-by-monolayer film formation by electrophoretic deposition in nonpolar solvents. <b>2012</b> , 28, 5295-301	24
746	Fabrication of Zinc Oxide Semiconductor Nanoparticles in the Apoferritin Cavity. <b>2012</b> , 12, 4130-4134	13
745	Drying and nondrying layer-by-layer assembly for the fabrication of sodium silicate/TiO2 nanoparticle composite films. <b>2012</b> , 28, 1816-23	9
744	A hierarchically assembled mesoporous ZnO hemisphere array and hollow microspheres for photocatalytic membrane water filtration. <b>2012</b> , 14, 7481-9	44
743	Photo-catalytic effect enhanced by the chemisorption of phenylethyl-mercaptan-assembled monolayers on Au-clusters/TiO2-anatase thin film. <b>2012</b> , 206, 4887-4891	2
742	Semiconductor Photocatalysis - Past, Present, and Future Outlook. <i>Journal of Physical Chemistry Letters</i> , <b>2012</b> , 3, 673-7	454
741	Surface plasmon resonance-mediated photocatalysis by noble metal-based composites under visible light. <i>Journal of Materials Chemistry</i> , <b>2012</b> , 22, 21337	412
740	New insights into the relationship between photocatalytic activity and photocurrent of TiO2/WO3 nanocomposite. <b>2012</b> , 433-434, 81-87	69
739	Low-temperature solvothermal synthesis of visible-light-responsive S-doped TiO2 nanocrystal. <b>2012</b> , 258, 4016-4022	76
738	Hierarchical TiO2/CdS "spindle-like" composite with high photodegradation and antibacterial capability under visible light irradiation. <b>2012</b> , 229-230, 209-16	79
737	Elaboration, charge-carrier lifetimes and activity of Pd-TiO2 photocatalysts obtained by gamma radiolysis. <b>2012</b> , 242, 34-43	47
736	Does a photocatalytic synergy in an anatase-rutile TiO2 composite thin-film exist?. <b>2012</b> , 18, 13048-58	41
735	Biocatalyzed artificial photosynthesis by hydrogen-terminated silicon nanowires. <b>2012</b> , 5, 2129-32, 2089	18
734	Atomic Layer Deposition of WO3 Thin Films using W(CO)6 and O3 Precursors. <b>2012</b> , 18, 245-248	44

733	A review of photocatalysis using self-organized TiO2 nanotubes and other ordered oxide nanostructures. <b>2012</b> , 8, 3073-103	533
732	CdS nanoparticles sensitization of Al-doped ZnO nanorod array thin film with hydrogen treatment as an ITO/FTO-free photoanode for solar water splitting. <b>2012</b> , 7, 593	29
731	Particle Networks from Powder Mixtures: Generation of TiO(2)-SnO(2) Heterojunctions via Surface Charge-Induced Heteroaggregation. <b>2012</b> , 116, 22967-22973	57
730	Solar Photoconversion Using Graphene/TiO2 Composites: Nanographene Shell on TiO2 Core versus TiO2 Nanoparticles on Graphene Sheet. <b>2012</b> , 116, 1535-1543	272
729	Molecular Metal Oxide Cluster-Surface Modified Titanium(IV) Dioxide Photocatalysts. <b>2012</b> , 65, 624	28
728	Efficient removal of methylene blue over composite-phase BiVO4 fabricated by hydrothermal control synthesis. <b>2012</b> , 136, 897-902	46
727	Persistent luminescence assisted photocatalytic properties of CaAl2O4:(Eu,Nd)/TiO2☑Ny and Sr4Al14O25:(Eu,Dy)/TiO2☑Ny. <b>2012</b> , 363-364, 129-133	12
726	Sodium chloride template synthesis of cubic tin dioxide hollow particles for lithium ion battery applications. <b>2012</b> , 4, 1537-42	67
725	ZnO/TiO2 coreBrush nanostructure: processing, microstructure and enhanced photocatalytic activity. <i>Journal of Materials Chemistry</i> , <b>2012</b> , 22, 5629	98
724	Facile Fabrication and High Photoelectric Properties of Hierarchically Ordered Porous TiO2. <b>2012</b> , 24, 3800-3810	53
723	Carbon quantum dots embedded with mesoporous hematite nanospheres as efficient visible light-active photocatalysts. <i>Journal of Materials Chemistry</i> , <b>2012</b> , 22, 8345	193
722	Synthesis of ZnO/CdS hierarchical heterostructure with enhanced photocatalytic efficiency under nature sunlight. <b>2012</b> , 14, 3615	161
721	Photocatalytic water purification using planar microreactor. 2012,	
720	Fabrication and photocatalytic properties of silicon nanowires by metal-assisted chemical etching: effect of H2O2 concentration. <b>2012</b> , 7, 663	49
719	Microfluidic photoelectrocatalytic reactors for water purification with an integrated visible-light source. <b>2012</b> , 12, 3983-90	72
718	CoFe2O4 <b>E</b> e3O4Magnetic Nanocomposites as Photocatalyst for the Degradation of Methyl Orange Dye. <b>2012</b> , 2012, 1-6	16
717	Photocatalytic Reduction and Oxidation of Water. <b>2012</b> , 235-259	
716	Carbon quantum dots/Ag3PO4 complex photocatalysts with enhanced photocatalytic activity and stability under visible light. <i>Journal of Materials Chemistry</i> , <b>2012</b> , 22, 10501	614

715	A survey of photocatalytic materials for environmental remediation. <b>2012</b> , 211-212, 3-29	681
714	Solvothermal synthesis and photocatalytic application of porous Au/TiO2 nanocomposites. <i>Journal of Materials Chemistry</i> , <b>2012</b> , 22, 11701	30
713	Advanced nanoarchitectures for solar photocatalytic applications. <b>2012</b> , 112, 1555-614	1888
712	The electrochemistry of nanostructured titanium dioxide electrodes. <b>2012</b> , 13, 2824-75	210
711	One-pot synthesis of nitrogen-doped TiO2 nanorods with anatase/brookite structures and enhanced photocatalytic activity. <b>2012</b> , 14, 7662	52
710	About the Nitrogen Location in Nanocrystalline N-Doped TiO2: Combined DFT and EXAFS Approach. <b>2012</b> , 116, 1764-1771	66
709	Enhanced Photocurrent Responses and Antiphotocorrosion Performance of CdS Hybrid Derived from Triple Heterojunction. <b>2012</b> , 116, 12829-12835	44
708	CVD Production of Doped Titanium Dioxide Thin Films. <b>2012</b> , 18, 89-101	31
707	Solvothermal synthesis of flower-like BiOBr microspheres with highly visible-light photocatalytic performances. <b>2012</b> , 111-112, 334-341	372
706	Visible-light-activation of TiO2 nanotube array by the molecular iron oxide surface modification. <b>2012</b> , 119-120, 74-80	19
7 <sup>0</sup> 5	Synthesis and photo activity of flower-like anatase TiO2 with {001} facets exposed. <b>2012</b> , 66, 308-310	10
704	Synthesis and photocatalytic activity of ferrites under visible light: A review. <b>2012</b> , 87, 1-14	536
703	Photoelectrocatalytic technologies for environmental applications. <b>2012</b> , 238, 41-52	189
702	Effects of oxygen vacancy and N-doping on the electronic and photocatalytic properties of Bi2MO6 (M=Mo, W). <b>2012</b> , 187, 103-108	64
701	Synthesis and photocatalytic performance of the efficient visible light photocatalyst AgAgCl/BiVO4. <b>2012</b> , 353-354, 22-28	118
700	Facile synthesis of Ag nanoparticles supported on TiO2 inverse opal with enhanced visible-light photocatalytic activity. <b>2012</b> , 520, 3515-3522	45
699	Fabrication and photocatalytic properties of novel ZnO/ZnAl2O4 nanocomposite with ZnAl2O4 dispersed inside ZnO network. <b>2012</b> , 58, 573-582	91
698	Facet-Mediated Photodegradation of Organic Dye over Hematite Architectures by Visible Light.  Angewandte Chemie, <b>2012</b> , 124, 182-186	5 58

697	Facet-mediated photodegradation of organic dye over hematite architectures by visible light.  Angewandte Chemie - International Edition, 2012, 51, 178-82	231
696	Interfacial nature of Ag nanoparticles supported on TiO2 photocatalysts. <b>2012</b> , 47, 824-832	44
695	Paramagnetic centers of photocatalysts based on nitrogen-doped titanium dioxide. 2013, 54, 373-377	7
694	Novel quasi-cube TiO2 nanoparticles as light-scattering layers for dye-sensitized solar cells. <b>2013</b> , 15, 1	9
693	Facile synthesis of MWCNTs/Ag3PO4: novel photocatalysts with enhanced photocatalytic activity under visible light. <b>2013</b> , 15, 1	15
692	Photoinduced Electron Transfer of ZnSAgInS2 Solid-Solution Semiconductor Nanoparticles: Emission Quenching and Photocatalytic Reactions Controlled by Electrostatic Forces. <b>2013</b> , 117, 15667-15676	16
691	Fast-generation of Ag3PO4 concave microcrystals from electrochemical oxidation of bulk silver sheet. <b>2013</b> , 15, 5070	27
690	Design of Advanced Photocatalytic Materials for Energy and Environmental Applications. 2013,	65
689	Effect of oxygen vacancy and Al-doping on the electronic and optical properties in SnO2. 2013, 428, 48-52	11
688	Enhanced photocatalytic performance of Fe-doped SnO2 nanoarchitectures under UV irradiation: synthesis and activity. <b>2013</b> , 48, 6404-6409	21
687	Synthesis of ZnO/CdSe hierarchical heterostructure with improved visible photocatalytic efficiency. <b>2013</b> , 274, 39-44	39
686	Self-Cleaning Materials Based on Solar Photocatalysis. <b>2013</b> , 167-190	5
685	Structural and Electronic Properties of Group 6 Transition Metal Oxide Clusters. 2013, 21-61	1
684	Self-Ordered Titanium Dioxide Nanotube Arrays: Anodic Synthesis and Their Photo/Electro-Catalytic Applications. <b>2013</b> , 6, 2892-2957	78
683	Photocatalytic Nanooxides: The Case of TiO2 and ZnO. <b>2013</b> , 245-266	2
682	Gold nanoparticle doped hollow SnO2 supersymmetric nanostructures for improved photocatalysis. <b>2013</b> , 1, 4097	38
681	A green and direct synthesis of graphene oxide encapsulated TiO2 core/shell structures with enhanced photoactivity. <b>2013</b> , 230, 279-285	73
68o	Microwave-assisted growth of WO3D.33H2O micro/nanostructures with enhanced visible light photocatalytic properties. <b>2013</b> , 15, 7904	32

679	Iron(III)-based metal-organic frameworks as visible light photocatalysts. <b>2013</b> , 135, 14488-91		413
678	Visible light-driven CdSe nanotube array photocatalyst. <b>2013</b> , 8, 230		14
677	Synthesis and characterization of g-C3N4/MoO3 photocatalyst with improved visible-light photoactivity. <b>2013</b> , 283, 25-32		175
676	Effect of pH on the Barrier Layer of TiO2Nanoporous Films Potentiostatically Grown in Aqueous Media Containing Fluoride Ions. <b>2013</b> , 160, C291-C297		10
675	Anion-Doped Mixed Metal Oxide Nanostructures Derived from Layered Double Hydroxide as Visible Light Photocatalysts. <b>2013</b> , 23, 2348-2356		75
674	Zinc oxysulfide ternary alloy nanocrystals: A bandgap modulated photocatalyst. <b>2013</b> , 102, 233110		19
673	Effect of Counter-ion and Solvent on the Morphology and Barrier Layer Properties of Nanoporous/Nanotubular TiO2Films Grown by Anodization in Fluoride Containing Media. <b>2013</b> , 160, C247-C252		4
672	Nitrogen-doped nickel oxide thin films for enhanced electrochromic applications. <b>2013</b> , 527, 26-30		33
671	Enhanced photoelectrocatalytic performance of titanium dioxide/carbon cloth based photoelectrodes by graphene modification under visible-light irradiation. <b>2013</b> , 263 Pt 2, 291-8		39
670	Effect of CoOOH loading on the photoelectrocatalytic performance of WO3 nanorod array film. <b>2013</b> , 284, 285-290		23
669	Preparation of highly photocatalytically active rutile titania nanorods decorated with anatase nanoparticles produced by a titanyl-oxalato complex solution. <b>2013</b> , 16, 2032-2038		5
668	Synthesis, characterization, and visible photocatalytic performance of Zn2GeO4 nanobelts modified by CdS quantum dots. <b>2013</b> , 218, 73-80		10
667	Preparation of Nanometric Mixed Crystals of TiO2 by TiCl4 and TiCl3. 2013, 457-458, 81-87		
666	Simultaneous induction of high level thermal and visible-light catalytic activities to titanium(IV) oxide by surface modification with cobalt(III) oxide clusters. <b>2013</b> , 15, 20313-9		21
665	Efficient visible light photocatalysis of Bi4TaO8Cl nanoparticles synthesized by solution combustion technique. <i>RSC Advances</i> , <b>2013</b> , 3, 14371	3.7	33
664	Analysis of visible-light-active Sn(II)-TiO2 photocatalysts. <b>2013</b> , 15, 6185-9		11
663	Hierarchical flake-like Bi2MoO6/TiO2 bilayer films for visible-light-induced self-cleaning applications. <b>2013</b> , 1, 6961		88
662	Tailored preparation of titania with controllable phases of anatase and brookite by an alkalescent hydrothermal route. <b>2013</b> , 201, 151-158		50

661	Nanosheet array assembled by TiO2 nanocrystallites with {116} facets parallel to the nanosheet surface. <b>2013</b> , 1, 225-228		29
660	Applications of Nanomaterial-Based Membranes in Pollution Control. 2013, 43, 2389-2438		18
659	ZnOlan heterostructured nanosheets for solar energy harvesting: computational studies based on hybrid density functional theory. <b>2013</b> , 1, 2231-2237		49
658	Semiconductor photocatalysismechanistic and synthetic aspects. <i>Angewandte Chemie - International Edition</i> , <b>2013</b> , 52, 812-47	16.4	597
657	Anodic formation of a thick three-dimensional nanoporous WO3 film and its photocatalytic property. <b>2013</b> , 27, 128-132		51
656	Preparation of materials in the presence of hydrogen peroxide: from discrete or "zero-dimensional" objects to bulk materials. <b>2013</b> , 42, 29-45		46
655	Halbleiterphotokatalyse Imechanistische und prparative Aspekte. <i>Angewandte Chemie</i> , <b>2013</b> , 125, 842-879	3.6	80
654	Mechanisms of Reactions Induced by Photocatalysis of Titanium Dioxide Nanoparticles. <b>2013</b> , 115-157		2
653	Facile Synthesis of Face Oriented ZnO Crystals: Tunable Polar Facets and Shape Induced Enhanced Photocatalytic Performance. <b>2013</b> , 117, 4597-4605		104
652	Modified TiO2 For Environmental Photocatalytic Applications: A Review. <b>2013</b> , 52, 3581-3599		1082
651	Modified Photocatalysts. <b>2013</b> , 103-143		4
650	Graphene oxide-CdS composite with high photocatalytic degradation and disinfection activities under visible light irradiation. <b>2013</b> , 250-251, 412-20		225
649	Facile in situ synthesis of a Bi/BiOCl nanocomposite with high photocatalytic activity. <b>2013</b> , 1, 3068		280
648	Titanate@TiO2 coreBhell nanobelts with an enhanced photocatalytic activity. <b>2013</b> , 1, 7738		23
647	Identification and Roles of the Active Species Generated on Various Photocatalysts. <b>2013</b> , 1-24		9
646	Design and Development of Active Titania and Related Photocatalysts. <b>2013</b> , 73-102		2
645	Wastewater Treatment Using Highly Functional Immobilized TiO2 Thin-Film Photocatalysts. <b>2013</b> , 179-	197	3
644	Sensitization of Titania Semiconductor: A Promising Strategy to Utilize Visible Light. <b>2013</b> , 199-240		5

643	Photoelectrocatalysis for Water Purification. <b>2013</b> , 241-270	3
642	Controlled synthesis of nitrogen-doped binary and ternary TiO2 nanostructures with enhanced visible-light catalytic activity. <b>2013</b> , 199, 271-279	10
641	Doping TiO2 with p-block elements: Effects on photocatalytic activity. <b>2013</b> , 14, 13-28	283
640	Plasmonic photocatalysis. <b>2013</b> , 76, 046401	942
639	Fabrication and photocatalytic properties of spheres-in-spheres ZnO/ZnAl2O4 composite hollow microspheres. <b>2013</b> , 268, 237-245	67
638	Experimental and theoretical investigation into the elimination of organic pollutants from solution by layered double hydroxides. <b>2013</b> , 140-141, 241-248	44
637	Donor Icceptor porphyrin functionalized Pt nano-assemblies for artificial photosynthesis: a simple and efficient homogeneous photocatalytic hydrogen production system. <b>2013</b> , 3, 2295	36
636	Combinatorial atmospheric pressure chemical vapor deposition of graded TiOEVOImixed-phase composites and their dual functional property as self-cleaning and photochromic window coatings. <b>2013</b> , 15, 309-19	47
635	Surface modification of titania powder P25 with phosphate and phosphonic acidseffect on thermal stability and photocatalytic activity. <b>2013</b> , 393, 335-9	21
634	The simple, template free synthesis of a Bi2S3-ZnO heterostructure and its superior photocatalytic activity under UV-A light. <b>2013</b> , 42, 5338-47	99
633	One-Pot Facile Synthesis of Cerium-Doped TiO2 Mesoporous Nanofibers Using Collagen Fiber As the Biotemplate and Its Application in Visible Light Photocatalysis. <b>2013</b> , 117, 9739-9746	78
632	Coupling photocatalysis and redox biocatalysis toward biocatalyzed artificial photosynthesis. <b>2013</b> , 19, 4392-406	104
631	A new heterojunction Ag3PO4/Cr-SrTiO3 photocatalyst towards efficient elimination of gaseous organic pollutants under visible light irradiation. <b>2013</b> , 134-135, 286-292	116
630	Tailored synthesis of mesoporous TiO2 hollow nanostructures for catalytic applications. <b>2013</b> , 6, 2082	186
629	Synergism between Fe2O3 and WO3 particles: Photocatalytic activity enhancement and reaction mechanism. <b>2013</b> , 367, 103-107	46
628	Loading Effect in Copper(II) Oxide Cluster-Surface-Modified Titanium(IV) Oxide on Visible- and UV-Light Activities. <b>2013</b> , 117, 23848-23857	61
627	Role of Interparticle Charge Transfers in Agglomerated Photocatalyst Nanoparticles:  Demonstration in Aqueous Suspension of Dye-Sensitized TiO2. <i>Journal of Physical Chemistry Letters</i> , <b>2013</b> , 4, 189-94	87
626	Preparation of TiO2, Ag-doped TiO2 nanoparticle and TiO2BBA-15 nanocomposites using simple aqueous solution-based chemical method and study of their photocatalytical activity. <b>2013</b> , 8, 462-479	13

625	The CNT modified white C3N4 composite photocatalyst with enhanced visible-light response photoactivity. <b>2013</b> , 42, 7604-13	206
624	Synthesis, Characterization, and Activity of Tin Oxide Nanoparticles: Influence of Solvothermal Time on Photocatalytic Degradation of Rhodamine B. <b>2013</b> , 02, 13-18	46
623	Synthesis and Photo-Catalytic Properties Characterization of Graphene/TiO2 Nanotube Composites. <b>2013</b> , 544, 21-24	
622	Manganese Oxide-Surface Modified Titanium (IV) Dioxide as Environmental Catalyst. <b>2013</b> , 3, 444-454	33
621	Photocatalytic Activity and Selectivity of ZnO Materials in the Decomposition of Organic Compounds. <b>2013</b> , 5, 3841-3846	19
620	Hierarchical TiO /V O Multifunctional Membrane for Water Purification. <b>2013</b> , 78, 1475-1482	12
619	PHOTOCATALYTIC ACTIVITY OF BISMUTH VANADATE FOR THE DEGRADATION OF ORGANIC COMPOUNDS. <b>2013</b> , 08, 1350007	26
618	- Ordered Mesoporous Carbons Prepared by a Soft-Templating Method. <b>2013</b> , 118-143	1
617	Enhancement of Photoelectrocatalysis Efficiency by Using Nanostructured Electrodes. 2014,	8
616	Preparation of layered titanate with interlayer cadmium sulfide particles for visible-light-assisted dye degradation. <i>RSC Advances</i> , <b>2014</b> , 4, 61960-61967	5
615	References. <b>2014</b> , 211-244	
614	Dipole moment-tuned packing of TiO2 nanocrystals into monolayer films by electrophoretic deposition. <b>2014</b> , 105, 113108	8
613	Semiconductor Photocatalysis for Atom-Economic Reactions. <b>2014</b> , 181-220	
612	First principles investigation of anion-controlled red shift in light absorption in ZnX ( $X = O$ , S, Se) nanocluster modified rutile TiO2. <b>2014</b> , 2, 18796-18805	10
611	Preparation and Photocatalytic Property of Cubic WO3. <b>2014</b> , 1081, 304-307	
610	Homogeneously distributed CdS nanoparticles in the sulphonated poly(ether ether ketone) membrane: preparation, characterisation and visible-light photocatalytic properties. <b>2014</b> , 29, A14-A19	3
609	Principles of Heterogeneous Photocatalysis. <b>2014</b> , 1-41	3
608	Synthesis of long-lived photogenerated charge carriers of Si-modified Fe2O3 and its enhanced visible photocatalytic activity. <b>2014</b> , 49, 331-337	11

607	Visible light photocatalytic performance of hierarchical BiOBr microspheres synthesized via a reactable ionic liquid. <b>2014</b> , 23, 151-158	25
606	Elucidation of important parameters of BiVO4 responsible for photo-catalytic O2 evolution and insights about the rate of the catalytic process. <b>2014</b> , 245, 124-132	52
605	A critical review of CO2 photoconversion: Catalysts and reactors. <b>2014</b> , 224, 3-12	474
604	Investigation of novel material for effective photodegradation of bezafibrate in aqueous samples. <b>2014</b> , 21, 5242-8	17
603	One-pot/self-template synthesis of mesostructured vanadium oxide embedded carbon nanofiber as a visible-light photocatalyst. <i>RSC Advances</i> , <b>2014</b> , 4, 5901	5
602	Searching for the formation of TiO2 mesoporous films with durable photoactivity by synergy of WO3 and sodium using a simple sputtering and annealing process. <b>2014</b> , 150-151, 354-362	2
601	Photocatalytic degradation of Brilliant Red M5B using four different nanocomposites (ZnFe2O4, porous ZnFe2O4, ZnFe2O4IIiO2, FeTiO3) coated on glass. <b>2014</b> , 20, 2964-2968	20
600	Facile template-free one-pot fabrication of ZnCo2O4 microspheres with enhanced photocatalytic activities under visible-light illumination. <b>2014</b> , 239, 192-199	60
599	One-dimensional titania nanostructures: Synthesis and applications in dye-sensitized solar cells. <b>2014</b> , 558, 1-19	40
598	Molecular-Scale Transition Metal Oxide Nanocluster Surface-Modified Titanium Dioxide as Solar-Activated Environmental Catalysts. <b>2014</b> , 118, 12077-12086	69
597	Electrospun Nanofibers for Energy and Environmental Applications. 2014,	52
596	The stabilization effect of surface capping on photocatalytic activity and recyclable stability of Ag3PO4. <b>2014</b> , 46, 138-141	20
595	Direct synthesis of novel vanadium oxide embedded porous carbon nanofiber decorated with iron nanoparticles as a low-cost and highly efficient visible-light-driven photocatalyst. <b>2014</b> , 417, 199-205	24
594	Effect of Al3+ substituted zinc ferrite on photocatalytic degradation of Orange I azo dye. <b>2014</b> , 279, 17-23	66
593	Facile ion-exchange synthesis of visible light active Sn-doped defect pyrochlore K0.51Sb2.67O6.26 and study of its photocatalytic activity. <i>Journal of Chemical Technology and Biotechnology</i> , <b>2014</b> , 89, 1833-184	1 <sup>13</sup>
592	One-pot hydrothermal synthesis of BiPO4/BiVO4 with enhanced visible-light photocatalytic activities for methylene blue degradation. <i>RSC Advances</i> , <b>2014</b> , 4, 10968	79
591	Green-Synthesized BiVO4 Oriented along {040} Facets for Visible-Light-Driven Ethylene Degradation. <b>2014</b> , 53, 2640-2646	61
590	Photocatalytic Coatings. <b>2014</b> , 413-423	3

589	Low temperature synthesis and photocatalytic properties of mesoporous TiO2 nanospheres. <b>2014</b> , 591, 52-57	29
588	Plasmonic goldBilver alloy on TiO2 photocatalysts with tunable visible light activity. <b>2014</b> , 156-157, 116-121	103
587	Improving the efficiency of hematite nanorods for photoelectrochemical water splitting by doping with manganese. <b>2014</b> , 6, 5852-9	153
586	Surface modification of metal oxides by polar molecules in a non-polar, polarizable solvent system. <b>2014</b> , 50, 5397-9	27
585	Significantly enhancement of photocatalytic performances via coreBhell structure of ZnO@mpg-C3N4. <b>2014</b> , 147, 554-561	188
584	Engineering BiOX (X = Cl, Br, I) nanostructures for highly efficient photocatalytic applications. <b>2014</b> , 6, 2009-26	861
583	Catalytic activity of gold nanoparticles supported on KNbO3 microcubes. <b>2014</b> , 224, 140-146	24
582	Low temperature crystallization of yttrium orthoferrite by organic acid-assisted solgel synthesis. <b>2014</b> , 114, 136-139	9
581	Enhanced photocatalytic activity and stability of interstitial Ga-doped CdS: Combination of experiment and calculation. <b>2014</b> , 224, 104-113	32
580	ZnO nanorods/Pt and ZnO nanorods/Ag heteronanostructure arrays with enhanced photocatalytic degradation of dyes. <i>RSC Advances</i> , <b>2014</b> , 4, 59009-59016	27
579	Pt/TiO2 Nanosheets Array Dominated by {001} Facets with Enhanced Photocatalytic Activity. <b>2014</b> , 27, 530-534	O
578	Investigation of photocatalytic degradation of clindamycin antibiotic by using nano-ZnO catalysts. <b>2014</b> , 31, 2014-2019	23
577	A new-type of semiconductor Na0.9Mg0.45Ti3.55O8: preparation, characterization and photocatalysis. <b>2014</b> , 2, 20358-20366	20
576	Surface decoration of WO3 architectures with Fe2O3 nanoparticles for visible-light-driven photocatalysis. <b>2014</b> , 16, 3289	63
575	Multi-electron oxygen reduction by a hybrid visible-light-photocatalyst consisting of metal-oxide semiconductor and self-assembled biomimetic complex. <i>Angewandte Chemie - International Edition</i> , 16.4 <b>2014</b> , 53, 13894-7	29
574	In situ gold-loaded titania photonic crystals with enhanced photocatalytic activity. <b>2014</b> , 2, 545-553	68
573	Solar light driven Rhodamine B degradation over highly active SiCIIIO2 nanocomposite. <i>RSC Advances</i> , <b>2014</b> , 4, 12918-12928	31
572	Synthesis of TiO2 with controllable ratio of anatase to rutile. <b>2014</b> , 2, 9291	49

571	Iron based photoanodes for solar fuel production. <b>2014</b> , 16, 11834-42	109
570	In situ environmental transmission electron microscopy study of oxidation of two-dimensional Ti3C2 and formation of carbon-supported TiO2. <b>2014</b> , 2, 14339	211
569	A ferroelectric photocatalyst for enhancing hydrogen evolution: polarized particulate suspension. <b>2014</b> , 16, 10408-13	74
568	Synthesis of small yolk@hell Fe3O4@TiO2 nanoparticles with controllable thickness as recyclable photocatalysts. <i>RSC Advances</i> , <b>2014</b> , 4, 8901	38
567	Effect of the composition of Ti alloy on the photocatalytic activities of Ti-based oxide nanotube arrays prepared by anodic oxidation. <b>2014</b> , 319, 181-188	12
566	Synthesis and Activity of Plasmonic Photocatalysts. <b>2014</b> , 6, 2456-2476	84
565	Solar photocatalytic activity of nano-ZnO supported on activated carbon or brick grain particles: Role of adsorption in dye degradation. <b>2014</b> , 486, 159-169	131
564	Adsorption and photocatalytic degradation of 2-CP in wastewater onto CS/CoFe®  nanocomposite synthesized using gamma radiation. <b>2014</b> , 114, 65-72	28
563	Preparation of highly photocatalytic active CdS/TiO2 nanocomposites by combining chemical bath deposition and microwave-assisted hydrothermal synthesis. <b>2014</b> , 218, 81-89	41
562	Effects of various TiO2 nanostructures and graphene oxide on photocatalytic activity of TiO2. <b>2014</b> , 279, 96-104	78
561	Enhancement of the photoelectrocatalytic activity of TiO2/ACF for ethylene removal by Ag nanoparticles synthesized by Fray radiolysis. <b>2014</b> , 27, 397-403	8
560	Fe2O3 decorated ZnO nanorod-assembled hollow microspheres: Synthesis and enhanced visible-light photocatalysis. <b>2014</b> , 135, 135-138	26
559	Template-free solvothermal synthesis of WO3/WO3ľH2O hollow spheres and their enhanced photocatalytic activity from the mixture phase effect. <b>2014</b> , 16, 7493-7501	52
558	Acetylene oligomerization on the surface of TiO2: a step forward in the in situ synthesis of nanostructured carbonaceous structures on the surface of photoactive oxides. <b>2014</b> , 2, 12247-12254	22
557	High valence 3p and transition metal based MOFs. <b>2014</b> , 43, 6097-115	339
556	Reduced graphene oxide modified highly ordered TiO2 nanotube arrays photoelectrode with enhanced photoelectrocatalytic performance under visible-light irradiation. <b>2014</b> , 16, 14800-7	82
555	A COST-EFFECTIVE MAGNETIC PHOTOCATALYST PALYGORSKITEIIO2EexOy WITH EXCELLENT PERFORMANCE FOR DYE PHOTODEGRADATION UNDER VISIBLE LIGHT. <b>2014</b> , 09, 1450063	
554	Nitrogen-doped titanium dioxide as visible-light-sensitive photocatalyst: designs, developments, and prospects. <b>2014</b> , 114, 9824-52	899

553	Understanding TiO2 photocatalysis: mechanisms and materials. 2014, 114, 9919-86	3646
552	A hierarchical nanostructured carbon nanofiber-In2S3 photocatalyst with high photodegradation and disinfection abilities under visible light. <b>2014</b> , 9, 1663-70	11
551	Investigation of the photoelectronic properties of nanocrystalline carbon- and nitrogen-doped titanium dioxide. <b>2014</b> , 69, 180-184	2
550	Cu2O/TiO2 heterostructure nanotube arrays prepared by an electrodeposition method exhibiting enhanced photocatalytic activity for CO2 reduction to methanol. <b>2014</b> , 46, 17-21	126
549	Fabrication of a visible-light-driven plasmonic photocatalyst of AgVO@AgBr@Ag nanobelt heterostructures. <b>2014</b> , 6, 5061-8	87
548	Coprecipitates Synthesis of CaIn2O4 and Its Photocatalytic Degradation of Methylene Blue by Visible Light Irradiation. <b>2014</b> , 53, 11720-11726	15
547	Novel SrAuInO: Synthesis, characterization and photocatalytic activity. <b>2014</b> , 75, 701-715	8
546	Semiconducting properties of ZnO/TiO2 composites by electrochemical measurements and their relationship with photocatalytic activity. <b>2014</b> , 140, 541-549	74
545	Enhanced photoabsorption properties of composites of Ti/TiO2 nanotubes decorated by Sb2S3 and improvement of degradation of hair dye. <b>2014</b> , 276, 96-103	38
544	Vertically aligned CdTe nanotube arrays on indium tin oxide for visible-light-driven photoelectrocatalysis. <b>2014</b> , 147, 17-21	18
543	Photoelectrocatalytic oxidation of Cu-EDTA complex and electrodeposition recovery of Cu in a continuous tubular photoelectrochemical reactor. <b>2014</b> , 239, 53-59	50
542	Mixed oxide semiconductors based on bismuth for photoelectrochemical applications. <b>2014</b> , 18, 1963-1971	10
541	Visible-light-driven photocatalytic properties of ZnO/ZnFe2O4 core/shell nanocable arrays. <b>2014</b> , 160-161, 408-414	126
540	Modern Electrochemical Methods in Nano, Surface and Corrosion Science. <b>2014</b> ,	3
539	Multi-Electron Oxygen Reduction by a Hybrid Visible-Light-Photocatalyst Consisting of Metal-Oxide Semiconductor and Self-Assembled Biomimetic Complex. <i>Angewandte Chemie</i> , <b>2014</b> , 126, 14114-14117 <sup>3.6</sup>	5
538	Detailed Characterization of Surface Ln-Doped Anatase TiO2 Nanoparticles by Hydrothermal Treatment for Photocatalysis and Gas Sensing Applications. <b>2015</b> , 1806, 25-30	
537	Multifunctional Single-Phase Photocatalysts: Extended Near Infrared Photoactivity and Reliable Magnetic Recyclability. <b>2015</b> , 5, 15511	26
536	Heterostructures Based on TiO2 and Silicon for Solar Hydrogen Generation. <b>2015</b> , 219-281	3

535	Facile Preparation of Silver Halide Nanoparticles as Visible Light Photocatalysts. <b>2015</b> , 5, 20	14
534	Degradation mechanism of hydrogen-terminated porous silicon in the presence and in the absence of light. <b>2015</b> , 5, 067125	6
533	Synthesis of Rod-Like g-C3N4/ZnS Composites with Superior Photocatalytic Activity for the Degradation of Methyl Orange. <b>2015</b> , 2015, 4108-4115	47
532	. 2015,	12
531	Improving the photocatalytic performance of polyimide by constructing an inorganic-organic hybrid ZnO-polyimide core⊠hell structure. <b>2015</b> , 406, 46-50	41
530	A nucleus-coupled electron transfer mechanism for TiO2-catalyzed water splitting. <b>2015</b> , 17, 16779-83	11
529	Visible-Light-Induced Self-Cleaning Property of Bi2Ti2O7-TiO2 Composite Nanowire Arrays. <b>2015</b> , 31, 5962-9	36
528	Time-dependent evolution of the Bi(3.64)Mo(0.36)O(6.55)/Bi2MoO6 heterostructure for enhanced photocatalytic activity via the interfacial hole migration. <b>2015</b> , 7, 11991-9	94
527	BiOBr visible-light photocatalytic films in a rotating disk reactor for the degradation of organics. <b>2015</b> , 3, 14801-14808	29
526	Photoelectrocatalytic activity of a hydrothermally grown branched Zno nanorod-array electrode for paracetamol degradation. <b>2015</b> , 291, 9-17	36
525	Photodeposition synthesis of a ZnO nanoporous layer. <i>RSC Advances</i> , <b>2015</b> , 5, 52998-53002 3.7	1
524	Modified titanium oxide (TiO2) nanocomposites and its array of applications: a review. <b>2015</b> , 97, 491-514	70
523	The layered double hydroxide route to Bi-Zn co-doped TiOlwith high photocatalytic activity under visible light. <b>2015</b> , 288, 158-67	50
522	Metal organic frameworks CAU-1 as new photocatalyst for photochemical vapour generation for analytical atomic spectrometry. <b>2015</b> , 30, 339-342	32
521	A new visible light active multifunctional ternary composite based on TiO2Ih2O3 nanocrystals heterojunction decorated porous graphitic carbon nitride for photocatalytic treatment of hazardous pollutant and H2 evolution. <b>2015</b> , 170-171, 195-205	140
520	Adsorption and photocatalytic performance of cuprous oxide/titania composite in the degradation of acid red B. <b>2015</b> , 33, 9-15	14
519	Synergistic photocatalytic hydrogen evolution over oxide nanosheets combined with photochemically inert additives. <b>2015</b> , 17, 5547-50	11
518	Effects of annealing temperature on the physicochemical, optical and photoelectrochemical properties of nanostructured hematite thin films prepared via electrodeposition method. <b>2015</b> , 69, 71-77	42

517	A solar-driven photocatalytic fuel cell with dual photoelectrode for simultaneous wastewater treatment and hydrogen production. <b>2015</b> , 3, 3416-3424	98
516	An efficient removal of methyl violet from aqueous solution by an AC-Bi/ZnO nanocomposite material. <i>RSC Advances</i> , <b>2015</b> , 5, 25857-25869	45
515	Photo-catalytic activity of BiVO4 thin-film electrodes for solar-driven water splitting. <b>2015</b> , 504, 266-271	48
514	Hierarchical flower-like Bi2WO6 hollow microspheres: facile synthesis and excellent catalytic performance. <i>RSC Advances</i> , <b>2015</b> , 5, 23080-23085	13
513	Ag2CO3/UiO-66(Zr) composite with enhanced visible-light promoted photocatalytic activity for dye degradation. <b>2015</b> , 299, 132-40	107
512	Contaminant effects on the photo-oxidation of greywater over titania film catalysts. <b>2015</b> , 7, 46-53	4
511	Achievements and Trends in Photoelectrocatalysis: from Environmental to Energy Applications. <b>2015</b> , 6, 415-441	143
510	UVIIisible light-activated Au@ pre-sulphated, monodisperse TiO2 aggregates for treatment of congo red and phthalylsulfathiazole. <b>2015</b> , 7, 187-195	5
509	Investigating the photo-oxidation of model indoor air pollutants using field asymmetric ion mobility spectrometry. <b>2015</b> , 312, 1-7	7
508	Aerobic oxidative CH/CH coupling of azaaromatics with indoles and pyrroles in the presence of TiO2 as a photocatalyst. <b>2015</b> , 17, 4401-4410	43
507	A short overview of the state of the art and perspectives on the main basic factors hindering the development of photocatalytic treatment of water. <b>2015</b> , 15, 1-10	7
506	Controllable synthesis porous Ag2CO3 nanorods for efficient photocatalysis. <b>2015</b> , 10, 193	23
505	One-pot facile synthesis of branched Ag-ZnO heterojunction nanostructure as highly efficient photocatalytic catalyst. <b>2015</b> , 353, 949-957	36
504	The synthesize of lanthanide doped BiVO4 and its enhanced photocatalytic activity. <b>2015</b> , 211, 25-30	17
503	Hot-Electron-Induced Highly Efficient O2 Activation by Pt Nanoparticles Supported on Ta2O5 Driven by Visible Light. <b>2015</b> , 137, 9324-32	117
502	Self-Template Synthesis of Porous Perovskite Titanate Solid and Hollow Submicrospheres for Photocatalytic Oxygen Evolution and Mesoscopic Solar Cells. <b>2015</b> , 7, 14859-69	55
501	Growth mechanism of ZnO nanorod/Fe3O4 nanoparticle composites and their photocatalytic properties. <b>2015</b> , 74, 71-73	7
500	Environmental Photochemistry Part III. <b>2015</b> ,	2

499	Synthesis and photocatalytic activity of ring-like anatase TiO2 with {001} facts exposed. 2015, 41, 8717-872	2 6
498	Photoelectrocatalytic decomposition of ethylene using TiO2/activated carbon fiber electrode with applied pulsed direct current square-wave potential. <b>2015</b> , 341, 61-68	14
497	Mesoporous TiO2@Ag3PO4 photocatalyst with high adsorbility and enhanced photocatalytic activity under visible light. <b>2015</b> , 70, 129-136	30
496	Solution plasma synthesis of Au nanoparticles for coating titanium dioxide to enhance its photocatalytic activity. <b>2015</b> , 583, 135-141	6
495	In situ formed Bi/BiOBrxI1-x heterojunction of hierarchical microspheres for efficient visible-light photocatalytic activity. <b>2015</b> , 17, 13347-54	61
494	Titaniallay heterostructures with solar photocatalytic applications. <b>2015</b> , 176-177, 278-287	64
493	Preparation of Bi2O3/g-C3N4 nanosheet pl junction for enhanced photocatalytic ability under visible light illumination. <b>2015</b> , 17, 1	26
492	Down-conversion photoluminescence sensitizing plasmonic silver nanoparticles on ZnO nanorods to generate hydrogen by water splitting photochemistry. <b>2015</b> , 106, 023114	14
491	Transient Absorption Spectroscopy of Anatase and Rutile: The Impact of Morphology and Phase on Photocatalytic Activity. <b>2015</b> , 119, 10439-10447	107
490	Enhanced visible-light photocatalytic performance of BiOBr/UiO-66(Zr) composite for dye degradation with the assistance of UiO-66. <i>RSC Advances</i> , <b>2015</b> , 5, 39592-39600	86
489	Magnetic iron oxide nanoparticles as long wavelength photoinitiators for free radical polymerization. <b>2015</b> , 6, 1918-1922	20
488	References. <b>2015</b> , 445-463	
487	Enhanced Photocatalytic Activity of the AgI/UiO-66(Zr) Composite for Rhodamine B Degradation under Visible-Light Irradiation. <b>2015</b> , 80, 1321-1328	47
486	Visible light caffeic acid degradation by carbon-doped titanium dioxide. <b>2015</b> , 31, 3627-34	36
485	Multifunctional radical-doped polyoxometalate-based host-guest material: photochromism and photocatalytic activity. <b>2015</b> , 54, 4345-50	118
484	Cleaning of olive mill wastewaters by visible light activated carbon doped titanium dioxide. <i>RSC Advances</i> , <b>2015</b> , 5, 85586-85591	11
483	Preparation, Characterization and Growth Mechanism of Dandelion-like TiO2 Nanostructures and their Application in Photocatalysis towards Reduction of Cr(VI). <b>2015</b> , 2, 3973-3987	9
482	Removal of methylene blue from wastewater under a low power irradiation source by Zn, Mn co-doped TiO2 photocatalysts. <i>RSC Advances</i> , <b>2015</b> , 5, 98166-98176	37

481	Capsule-like CdS-modified TiO2 nanocomposites with enhanced photodegradation under visible light irradiation. <b>2015</b> , 10, 157-160	5
480	Efficient COD Removal Coinciding with Dye Decoloration by Five-Layer Aurivillius Perovskites under Sunlight-Irradiation. <b>2015</b> , 3, 2900-2908	21
479	Highly transparent poly(2-ethyl-2-oxazoline)-TiO2 nanocomposite coatings for the conservation of matte painted artworks. <i>RSC Advances</i> , <b>2015</b> , 5, 84879-84888	26
478	Resolving the Controversy about the Band Alignment between Rutile and Anatase: The Role of OH <b>/</b> H+ Adsorption. <b>2015</b> , 119, 21952-21958	42
477	A study of dielectric, optical and magnetic characteristics of maghemite nanocrystallites. <b>2015</b> , 164, 183-187	6
476	Toward NIR driven photocatalyst: Fabrication, characterization, and photocatalytic activity of <code>#NaYF4:Yb(3+),Tm(3+)/g-C3N4</code> nanocomposite. <b>2015</b> , 460, 264-72	37
475	GlycineBitrate-based solution-combustion synthesis of SrTiO3. <b>2015</b> , 652, 496-502	18
474	Metal oxide semiconductors for dye degradation. <b>2015</b> , 72, 220-228	19
473	Antibacterial surfaces based on functionally graded photocatalytic Fe3O4@TiO2 coreShell nanoparticle/epoxy composites. <i>RSC Advances</i> , <b>2015</b> , 5, 105416-105421	14
472	Synthesis and visible photocatalytic activity of new photocatalyst MBi2O4(M = Cu, Zn). <b>2015</b> , 26, 1866-1873	18
471	Hydrogen production by photoelectrolysis of aqueous solutions of phenol using mixed oxide semiconductor films of BiŊbŊŊ (M = Al, Fe, Ga, In) as photoanodes. <b>2015</b> , 252, 150-156	7
470	Titanium dioxide encapsulation of supported Ag nanoparticles on the porous silica bead for increased photocatalytic activity. <b>2015</b> , 326, 82-90	22
469	Thermal decomposition approach for the synthesis of CdSIIiO2 nanocomposites and their catalytic activity towards degradation of rhodamine B and reduction of Cr(VI). <b>2015</b> , 41, 2160-2179	32
468	Facile synthesis of InVO4/TiO2 heterojunction photocatalysts with enhanced photocatalytic properties under UV $\square$ is irradiation. <b>2015</b> , 299, 152-158	38
467	A green and direct synthesis of photosensitized CoS2graphene/TiO2 hybrid with high photocatalytic performance. <b>2015</b> , 22, 264-271	31
466	Zinc oxide based photocatalysis: tailoring surface-bulk structure and related interfacial charge carrier dynamics for better environmental applications. <i>RSC Advances</i> , <b>2015</b> , 5, 3306-3351	566
465	Superior optical properties of Fe3+W18O49 nanoparticles prepared by solution combustion synthesis. <b>2015</b> , 39, 1196-1201	15
464	Layered KTiNbO5 photocatalyst modified with transitional metal ions (Mn2 +, Ni2 +): Investigation of microstructure and photocatalytic reaction pathways for the oxidation of dimethyl sulfide and ethyl mercantan 2015, 270, 154-162	17

# (2016-2015)

463	N-doped TiO2 nanotubes coated with a thin TaOxNy layer for photoelectrochemical water splitting: dual bulk and surface modification of photoanodes. <b>2015</b> , 8, 247-257	131
462	Synthesis of Ag3PO4AgBr with a novel heterostructure, and its photocatalytic properties. <b>2015</b> , 41, 5137-5147	13
461	First-Transition Metal OxocomplexBurface-Modified Titanium(IV) Oxide for Solar Environmental Purification. <b>2016</b> ,	
460	Mechanisms in Heterogeneous Photocatalysis: Titania under UV and Visible Light Illumination. <b>2016</b>	3
459	Typical NonTiO2-Based Visible-Light Photocatalysts. <b>2016</b> ,	3
458	Efficient Solar-Induced Photoelectrochemical Response Using Coupling Semiconductor TiOEInO Nanorod Film. <b>2016</b> , 9,	11
457	Preparation of TiOEDecorated Boron Particles by Wet Ball Milling and their Photoelectrochemical Hydrogen and Oxygen Evolution Reactions. <b>2016</b> , 9,	17
456	Facile Synthesis of g-CNINanosheets/ZnO Nanocomposites with Enhanced Photocatalytic Activity in Reduction of Aqueous Chromium(VI) under Visible Light. <b>2016</b> , 6,	89
455	A review on removal of elemental mercury from flue gas using advanced oxidation process: Chemistry and process. <b>2016</b> , 112, 199-250	120
454	Visible light photocatalysis by metal-to-metal charge transfer for degradation of methyl orange. <b>2016</b> , 4, 12479-12486	9
453	Design of Novel Visible Light Active Photocatalyst Materials: Surface Modified TiO2. <b>2016</b> , 28, 5425-46	119
452	Construction of visible light-induced renewable electrode for monitoring of living cells. <b>2016</b> , 781, 371-376	3
45 <sup>1</sup>	Poly(3,4-ethylenedioxythiophene) (PEDOT) infused TiO2 nanofibers: the role of hole transport layer in photocatalytic degradation of phenazopyridine as a pharmaceutical contaminant. <i>RSC Advances</i> , <b>2016</b> , 6, 113884-113892	12
450	The Application of Nano-TiO Photo Semiconductors in Agriculture. <b>2016</b> , 11, 529	52
449	Electrodeposition of composite FeIIiO2 coatings from methanesulfonate electrolyte. <b>2016</b> , 52, 532-537	10
448	Monitoring Photochemical Reaction Pathways of Tungsten Hexacarbonyl in Solution from Femtoseconds to Minutes. <b>2016</b> , 120, 13161-13168	17
447	Amplified visible light photocatalytic activity of mesoporous TiO2/ZnPc hybrid by cascade Mie light scattering. <b>2016</b> , 227, 169-175	6
446	l-lysine monohydrate mediated facile and environment friendly synthesis of SnO2 nanoparticles and their prospective applications as a catalyst for the reduction and photodegradation of aromatic compounds. <b>2016</b> , 4, 2976-2989	20

445	Surface Modification or Doping of WO3 for Enhancing the Photocatalytic Degradation of Organic Pollutant Containing Wastewaters: A Review. <b>2016</b> , 855, 105-126	11
444	Synthesis, characterization and optical properties of gadolinium doped copper ferrite nanoparticles prepared by novel solgel method. <b>2016</b> , 27, 6313-6317	
443	Microstructure and charge trapping assessment in highly reactive mixed phase TiO2 photocatalysts. <b>2016</b> , 192, 242-252	68
442	Magnetic double-tartaric bridging mono-lanthanide substituted phosphotungstates with photochromic and switchable luminescence properties. <b>2016</b> , 4, 5424-5433	58
441	Graphene oxide with zinc partially substituted magnetite (GO⊞e1⊠ZnxOy) for the UV-assisted heterogeneous Fenton-like reaction. <i>RSC Advances</i> , <b>2016</b> , 6, 44749-44757 3.7	7
440	Formation of BiOCl/Bi2O3 and Related Materials for Efficient Visible-Light Photocatalysis. <b>2016</b> , 405-427	
439	Morphology Control and Photocatalysis Enhancement by in Situ Hybridization of Cuprous Oxide with Nitrogen-Doped Carbon Quantum Dots. <b>2016</b> , 32, 9418-27	76
438	Understanding the synergistic between optimum dopant loading and charge transfer kinetics in platinum-mediated nanostructured hematite thin films. <b>2016</b> , 66, 249-257	11
437	Hydrazine-based synergistic Ti(III)/N doping of surfactant-templated TiO2 thin films for enhanced visible light photocatalysis. <b>2016</b> , 182, 382-393	18
436	Enhanced photocatalytic activity and persistent luminescence in Zn2GeO4:Mn2+ by Eu3+ doping. <b>2016</b> , 30, 1650305	4
435	Investigation of adsorption and photocatalytic activities of in situ cetyltrimethylammonium bromide-modified Bi/BiOCl heterojunction photocatalyst for organic contaminants removal. <i>RSC Advances</i> , <b>2016</b> , 6, 93309-93317	18
434	Photocatalytic Properties of All Four Polymorphs of Nanostructured Iron Oxyhydroxides. <b>2016</b> , 2, 1047-1054	25
433	The effect of silver nanoparticles/graphene-coupled TiO2 beads photocatalyst on the photoconversion efficiency of photoelectrochemical hydrogen production. <b>2016</b> , 27, 435405	14
432	Enhanced photoelectrochemical water splitting efficiency: Increasing the photo anodell properties by doping on the fluorine doped tin oxide glass surface. <b>2016</b> , 42, 458-472	3
431	Studies on structural defects in bare, PVP capped and TPPO capped copper oxide nanoparticles by positron annihilation lifetime spectroscopy and their impact on photocatalytic degradation of 3.7 rhodamine B. <i>RSC Advances</i> , <b>2016</b> , 6, 74812-74821	22
430	Sonochemical Synthesis of Zinc Sulfide Photocatalysts and Their Environmental Applications. <b>2016</b> , 867-899	
429	Synergistic Photocatalysis-Catalytic Peroxidation of BiOBr/H2O2 System for 4-Chlorophenol Degradation. <b>2016</b> , 1, 1000-1003	6
428	ZnS@g-C3N4 Composite Photocatalysts: In Situ Synthesis and Enhanced Visible-Light Photocatalytic Activity. <b>2016</b> , 146, 2185-2192	21

### (2016-2016)

427	obtained by plasma electrolytic oxidation. <b>2016</b> , 305, 192-199		24
426	Charge Transfer Reductive Doping of Mesoporous TiO Photoelectrodes - Impact of Electrolyte Composition and Film Morphology. <b>2016</b> , 120, 27882-27894		11
425	Photoelectrocatalytic degradation of benzoic acid using immobilized tungsten trioxide photocatalyst. <b>2016</b> , 183, 439-446		13
424	Nitrite Reduction Enhancement on Semiconducting Electrode Decorated with Copper(II) Aspirinate Complex. <b>2016</b> , 7, 486-494		1
423	Characterization of expanded graphene nanosheet as additional material and improved performances for electric double layer capacitors. <b>2016</b> , 43, 53-60		14
422	Magnetically recoverable Fe 3 O 4-ZnO/AOT nanocomposites: Synthesis of a corellhell structure via a novel and mild route for photocatalytic degradation of toxic dyes. <b>2016</b> , 223, 1133-1142		30
421	ZrxCo0.8Ni0.2NFe2O4-graphene nanocomposite for enhanced structural, dielectric and visible light photocatalytic applications. <b>2016</b> , 42, 15747-15755		20
420	ZnWO4/Ag3PO4 composites with an enhanced photocatalytic activity and stability under visible light. <i>RSC Advances</i> , <b>2016</b> , 6, 114818-114824	3.7	7
419	In situ growth of small Au nanoparticles on ZnO nanorods via ultrasonic irradiation toward super-enhanced catalytic activity. <i>RSC Advances</i> , <b>2016</b> , 6, 107433-107441	3.7	15
418	Application des process de des des des des des des des des d		3
417	Photoelectrochemical determination of Pb2+ ions by using TiO2 nanorod arrays grown on FTO substrates via a facile two-stage hydrothermal route. <b>2016</b> , 27, 8455-8463		10
416	Hybrid nanostructures of TiO2 nanorod array/Cu2O with a CH3NH3PbI3 interlayer for enhanced photocatalytic activity and photoelectrochemical performance. <i>RSC Advances</i> , <b>2016</b> , 6, 57695-57700	3.7	5
415	Visible-Light Induced Self-Powered Sensing Platform Based on a Photofuel Cell. <b>2016</b> , 88, 6140-4		58
414	Syntheses, structures and properties of two new 3-D vanadoborates based on V O B clusters. <b>2016</b> , 684, 537-543		6
413	Synthesis, characterization, and investigation of magnetic and photocatalytic property of CuFe2\( \text{ULaxO4}\) nanoparticles. <b>2016</b> , 27, 9526-9530		3
412	Preparation of Visible Light Active Ag- and N-Doped KVMoO6: Photodegradation of Methylene Blue. <b>2016</b> , 44, 1584-1590		3
411	EPR Study of TiO2 (Rutile) Doped with Vanadium. <b>2016</b> , 47, 479-485		5
410	Where Do Photogenerated Holes Go in Anatase:Rutile TiO2? A Transient Absorption Spectroscopy Study of Charge Transfer and Lifetime. <b>2016</b> , 120, 715-23		101

409	Photocatalytic degradation of gallic acid over CuOlliO2 composites under UV/Vis LEDs irradiation. <b>2016</b> , 521, 140-148		57
408	Microwave-assisted polyol synthesis and characterization of pvp-capped cds nanoparticles for the photocatalytic degradation of tartrazine. <b>2016</b> , 74, 387-396		43
407	Heterogeneous photocatalytic studies of analgesic and non-steroidal anti-inflammatory drugs. <b>2016</b> , 510, 134-155		70
406	Enhanced photocatalytic activity of La-substituted BiFeO 3 nanostructures on the degradation of phenol red. <b>2016</b> , 165, 205-209		40
405	Synthesis and photocatalytic activity of BiOBr nanosheets with tunable exposed {0 1 0} facets. <b>2016</b> , 188, 283-291		132
404	A hybrid organicIhorganic layered TiO2 based nanocomposite for sunlight photocatalysis. <i>RSC Advances</i> , <b>2016</b> , 6, 18538-18541	3.7	8
403	Preparation and characterization of TilnVO6-nanomaterial using precipitation method and its multi applications. <b>2016</b> , 27, 2488-2503		7
402	The accelerating effect of silver ion on the degradation of methyl orange in Cu2O system. <b>2016</b> , 512, 74-84		9
401	Environmental Applications of Interfacial Materials with Special Wettability. <b>2016</b> , 50, 2132-50		197
400	Incorporation of NØnO/CdS/Graphene oxide composite photocatalyst for enhanced photocatalytic activity under visible light. <b>2016</b> , 670, 198-209		80
399	Plasmonic and passivation effects of Au decorated RGO@CdSe nanofilm uplifted by CdSe@ZnO nanorods with photoelectrochemical enhancement. <b>2016</b> , 21, 185-197		32
398	Study of the photocurrent in a photocatalytic fuel cell for wastewater treatment and the effects of TiO2 surface morphology to the apportionment of the photocurrent. <b>2016</b> , 192, 319-327		18
397	High-performance dye-sensitized solar cell using dimensionally controlled titania synthesized at sub-zero temperatures. <i>RSC Advances</i> , <b>2016</b> , 6, 23459-23466	3.7	9
396	Volatile Hexavalent Oxo-amidinate Complexes: Molybdenum and Tungsten Precursors for Atomic Layer Deposition. <b>2016</b> , 28, 1907-1919		33
395	Hierarchical photocatalysts. <b>2016</b> , 45, 2603-36		1216
394	Enhanced photocatalytic activity of hydrothermally grown BiFeO3 nanostructures and role of catalyst recyclability in photocatalysis based on magnetic framework. <b>2016</b> , 122, 1		22
393	Photocatalytic hydrogen evolution from water splitting using Cu doped ZnS microspheres under visible light irradiation. <b>2016</b> , 89, 18-26		100
392	Photoelectrocatalytic hydrogen generation and simultaneous degradation of organic pollutant via CdSe/TiO2 nanotube arrays. <b>2016</b> , 362, 490-497		69

# (2017-2016)

391	A hierarchically porous anatase TiO2 coated-WO3 2D IO bilayer film and its photochromic properties. <b>2016</b> , 52, 892-5	20
390	N2/Ar plasma induced doping of ordered mesoporous TiO2 thin films for visible light active photocatalysis. <b>2016</b> , 220, 120-128	48
389	Research progress on iron oxide-based magnetic materials: Synthesis techniques and photocatalytic applications. <b>2016</b> , 42, 9-34	125
388	Efficient plasma-assisted approach in nanostructure fabrication of tungsten. <b>2016</b> , 89, 78-84	9
387	Combination of photoelectrocatalysis and ozonation: A novel and powerful approach applied in Acid Yellow 1 mineralization. <b>2016</b> , 180, 161-168	48
386	Hydrogen production and simultaneous photoelectrocatalytic pollutant oxidation using a TiO2/WO3 nanostructured photoanode under visible light irradiation. <b>2016</b> , 765, 188-196	27
385	Enhancement of durable photocatalytic properties of cotton/polyester fabrics using TiO2/SiO2 via one step sonosynthesis. <b>2017</b> , 46, 1633-1655	9
384	A review on g-C 3 N 4 -based photocatalysts. <b>2017</b> , 391, 72-123	1687
383	Hybrid (Organic/Inorganic) Electrodes from Bacterially Precipitated CdS for PEC/Storage Applications. <b>2017</b> , 121, 3734-3743	10
382	Sunlight responsive new Sillā-Aurivillius A1X1 hybrid layered oxyhalides with enhanced photocatalytic activity. <b>2017</b> , 161, 197-205	18
381	Ultraviolet Radiation Induced Dopant Loss in a TiO2 Photocatalyst. <i>ACS Catalysis</i> , <b>2017</b> , 7, 1485-1490 13.1	13
380	Photoelectrocatalytic activity of immobilized Yb doped WO 3 photocatalyst for degradation of methyl orange dye. <b>2017</b> , 26, 440-447	30
379	Molecular adsorption of hydrogen peroxide on N- and Fe-doped titania nanoclusters. 2017, 407, 121-129	2
378	Enriched photoelectrocatalytic degradation and photoelectric performance of BiOI photoelectrode by coupling rGO. <b>2017</b> , 208, 22-34	156
377	Visible-Light Driven Photocatalytic Degradation of Organic Dyes over Ordered Mesoporous CdxZn1⊠S Materials. <b>2017</b> , 121, 5137-5144	46
376	SnO2IIiO2 structures and the effect of CuO, CoO metal oxide on photocatalytic hydrogen production. <i>Journal of Chemical Technology and Biotechnology</i> , <b>2017</b> , 92, 1531-1539	35
375	Thermal-frequency dependence study of the sub-band localized states effect in Sb-doped SnO2 based sol-gel thin films. <b>2017</b> , 632, 66-72	26
374	UV and visible light synergetic photodegradation using rutile TiO nanorod arrays based on a p-n Junction. <b>2017</b> , 46, 4296-4302	14

373	A simple preparation method and characterization of B and N co-doped TiO 2 nanotube arrays with enhanced photoelectrochemical performance. <b>2017</b> , 413, 284-291		41
372	Layer-by-layer assembled photocatalysts for environmental remediation and solar energy conversion. <b>2017</b> , 32, 1-20		26
371	Vapor Phase Fabrication of Nanoheterostructures Based on ZnO for Photoelectrochemical Water Splitting. <b>2017</b> , 4, 1700161		24
370	Fabrication of metal/semiconductor nanocomposites by selective laser nano-welding. <b>2017</b> , 9, 7012-7015		17
369	ZnO/CdS nanorod arrays decorated by layered double hydroxides for efficient solar water oxidation. <b>2017</b> , 41, 1781-1789		9
368	Fabrication and characterization of photoelectrochemically-active Sb-doped Snx-W(100-x)%-oxide anodes: Towards the removal of organic pollutants from wastewater. <b>2017</b> , 416, 318-328		14
367	Iron waste as an effective depend on TiO2 for photocatalytic degradation of dye waste water. <b>2017</b> , 140, 197-204		8
366	Photoelectrochemical Degradation of Organic Compounds Coupled with Molecular Hydrogen Generation Using Electrochromic TiO Nanotube Arrays. <b>2017</b> , 51, 6590-6598		88
365	Synthesis and excellent visible light photocatalysis performance of magnetic reduced graphene oxide/ZnO/ZnFe2O4 composites. <i>RSC Advances</i> , <b>2017</b> , 7, 23246-23254	7	28
364	A Simple Method for the Electrodeposition of WO3 in TiO2 Nanotubes: Influence of the Amount of Tungsten on Photoelectrocatalytic Activity. <b>2017</b> , 8, 115-121		12
363	Water Oxidation Kinetics of Accumulated Holes on the Surface of a TiO2 Photoanode: A Rate Law Analysis. <i>ACS Catalysis</i> , <b>2017</b> , 7, 4896-4903	3.1	76
362	Fabrication of Ag 2 CO 3 /SrCO 3 Rods with Highly Efficient Visible-light Photocatalytic Activity. <b>2017</b> , 46, 312-316		8
361	Photoelectrochemical sensitive detection of insulin based on CdS/polydopamine co-sensitized WO nanorod and signal amplification of carbon nanotubes@polydopamine. <b>2017</b> , 96, 345-350		52
360	Photoeletrocatalytic degradation of gaseous acetone using electrical glassfiber filter coated with nano-sized TiO2 photoelectrocatalyst. <b>2017</b> , 77, 187-195		5
359	Preparation of porous CuO films from Cu(NO3)2 aqueous solutions containing poly(vinylpyrrolidone) and their photocathodic properties. <i>RSC Advances</i> , <b>2017</b> , 7, 18014-18018	7	5
358	Multifunctional Gadolinium-Doped Mesoporous TiO Nanobeads: Photoluminescence, Enhanced Spin Relaxation, and Reactive Oxygen Species Photogeneration, Beneficial for Cancer Diagnosis and Treatment. <b>2017</b> , 13, 1700349		43
357	Studies of Nanosized Iron-Doped TiO2 Photocatalysts by Spectroscopic Methods. <b>2017</b> , 48, 447-459		9
356	Reticulated ZnO Photocatalyst: Efficiency Enhancement in Degradation of Acid Red 88 Azo Dye by Catalyst Surface Cleaning. <b>2017</b> , 204, 705-710		9

### (2017-2017)

355	A novel ternary CuO decorated Ag3AsO4/GO hybrid as a Z-scheme photocatalyst for enhanced degradation of phenol under visible light. <b>2017</b> , 41, 1380-1389	19
354	Enhanced photocatalytic hydrogen generation and photostability of ZnO nanoparticles obtained via green synthesis. <b>2017</b> , 42, 5125-5131	53
353	Visible light photocatalytic and magnetic properties of Nd doped Bi2Fe4O9 powders. <b>2017</b> , 28, 4371-4377	5
352	A TiO2-nanotubes-based coil-type microreactor for highly efficient photoelectrocatalytic degradation of organic compounds. <b>2017</b> , 47, 384-390	10
351	Highly Luminescent WS Quantum Dots/ZnO Heterojunctions for Light Emitting Devices. 2017, 9, 558-565	75
350	Photocatalytic degradation of a model textile dye using Carbon-doped titanium dioxide and visible light. <b>2017</b> , 20, 71-77	40
349	A Review on Ferrate(VI) and Photocatalysis as Oxidation Processes for the Removal of Organic Pollutants in Water and Wastewater. <b>2017</b> , 331-390	3
348	Synthesis and photocatalysis of flaky flower TiO 2 with sphere structure. <b>2017</b> , 84, 283-289	4
347	Efficient photo-catalytic oxidative degradation of organic dyes using CuInSe2/TiO2 hybrid hetero-nanostructures. <b>2017</b> , 349, 73-90	16
346	Synthesis and application of barium ferrite/activated carbon composite as an effective solar photocatalyst for discoloration of organic dye contaminants in wastewater. <b>2017</b> , 5, 3822-3827	19
345	High efficiency for H2 evolution and NO removal over the Ag nanoparticles bridged g-C3N4 and WS2 heterojunction photocatalysts. <b>2017</b> , 219, 467-478	66
344	Visible light-driven photoelectrocatalysis coupling with electroenzymatic process for degradation of chloramphenicol. <b>2017</b> , 330, 1380-1389	25
343	CdS nanoparticles loaded on porous poly-melamineformaldehyde polymer for photocatalytic dye degradation. <b>2017</b> , 43, 5083-5090	6
342	Synthesis of visible light active Gd3+-substituted ZnFe2O4 nanoparticles for photocatalytic and antibacterial activities. <b>2017</b> , 132, 1	24
341	Nanocrystalline ZnOBnO2 mixed metal oxide powder: microstructural study, optical properties, and photocatalytic activity. <b>2017</b> , 84, 274-282	14
340	WO3 nanofibers on ACF by electrospun for photo-degradation of phenol solution. <b>2017</b> , 24, 1275-1280	4
339	Photoelectrocatalytic degradation of pharmaceutical carbamazepine using Sb-doped Sn80%-W20%-oxide electrodes. <b>2017</b> , 188, 52-59	24
338	A review: Effect of nanostructures on photocatalytic CO 2 conversion over metal oxides and compound semiconductors. <b>2017</b> , 20, 163-177	62

337	Solar Photocatalytic Water Oxidation and Purification on ZIF-8-Derived CNIZnO Composites. <b>2017</b> , 31, 2138-2143	22
336	Enhanced piezo/solar-photocatalytic activity of Ag/ZnO nanotetrapods arising from the coupling of surface plasmon resonance and piezophototronic effect. <b>2017</b> , 102, 27-33	49
335	Influence of surface metallic silver deposit and surface fluorination on the photocatalytic activity of rutile TiO2 for the degradation of crystal violet a cationic dye under UV light irradiation. <b>2017</b> , 10, 1-13	30
334	Advances in Photocatalytic Disinfection. 2017,	18
333	Rare earth oxides in zirconium dioxide: How to turn a wide band gap metal oxide into a visible light active photocatalyst. <b>2017</b> , 26, 270-276	45
332	Study on Structural, Multiferroic, Optical and Photocatalytic Properties of Ferroelectromagnetic Nanoparticles: Bi0.9Ba0.1Fe0.8Ti0.2O3. <b>2017</b> , 30, 431-439	3
331	Energetic states in SnO2IIiO2 structures and their impact on interfacial charge transfer process. <b>2017</b> , 52, 260-275	29
330	Ultrathin graphitic C3N4 nanosheet as a promising visible-light-activated support for boosting photoelectrocatalytic methanol oxidation. <b>2017</b> , 203, 108-115	179
329	Photoelectrocatalytic Materials for Water Disinfection. <b>2017</b> , 199-219	1
328	Electrodeposition of thin cadmium sulfide films from Na2SO3-based electrolyte. <b>2017</b> , 90, 1225-1229	5
327	Synthesis and Catalytic Applications of Non-Metal Doped Mesoporous Titania. <b>2017</b> , 5, 15	50
326	Impact of Ni Substitution on Structural, Electrical and Thermoelectrical Properties of Zinc Alluminium Chromites Synthesized by sol-gel Route and their Photocatalytic Investigation. <b>2017</b> , 20, 1445-1453	5
325	An Inverse Opal Structured Halide Perovskite Photocatalyst. <b>2018</b> , 2018, 2350-2355	28
324	Advances in the Development of Novel Photocatalysts for Detoxification. 2018, 283-327	1
323	Solar Photochemical Splitting of Water. <b>2018</b> , 365-391	
322	Efficient and Cost-effective Photoelectrochemical Degradation of Dyes in Wastewater over an Exfoliated Graphite-MoO3 Nanocomposite Electrode. <b>2018</b> , 9, 623-631	22
321	Identifying the key obstacle in photocatalytic oxygen evolution on rutile TiO2. <b>2018</b> , 1, 291-299	131
320	Determination of the Energy Levels of Paramagnetic Centers in the Band Gap of Nanostructured Oxide Semiconductors Using EPR Spectroscopy. <b>2018</b> , 122, 10248-10254	18

319	Aqueous synthesis of Z-scheme photocatalyst powders and thin-film photoanodes from earth abundant elements. <b>2018</b> , 6, 2606-2615	7
318	Understanding the degradation pathways of oxalic acid in different photocatalytic systems: Towards simultaneous photocatalytic hydrogen evolution. <b>2018</b> , 366, 81-90	16
317	Exploration of the evolution of nanotechnology from a patent co-classification perspective. <b>2018</b> , 7, 233-245	4
316	Robust sensitizer-assisted platinized titanium dioxide in photocatalytic removal of 4-chlorophenol in water: Light tunable sensitizer. <b>2018</b> , 358, 100-110	1
315	Photonic Fano Resonance of Multishaped Cu2O Nanoparticles on ZnO Nanowires Modulating Efficiency of Hydrogen Generation in Water Splitting Cell. <b>2018</b> , 6, 6590-6598	18
314	Sheet-like orthorhombic MoO3 nanostructures prepared via hydrothermal approach for visible-light-driven photocatalytic application. <b>2018</b> , 44, 1647-1660	10
313	High photocatalytic activities of zinc oxide nanotube arrays modified with tungsten trioxide nanoparticles. <b>2018</b> , 39, 54-62	13
312	Functional Materials and Systems for Rewritable Paper. <b>2018</b> , 30, e1705310	109
311	Multi-applicative tetragonal TiO2/SnO2 nanocomposites for photocatalysis and gas sensing. <b>2018</b> , 115, 127-136	46
310	Synergistic effect of PANI and NiFe2O4 for photocatalytic hydrogen evolution under visible light. <b>2018</b> , 43, 2121-2129	33
309	Synthesis of TiO2@Fe2O3 corelhell heteronanostructures by thermal decomposition approach and their application towards sunlight-driven photodegradation of rhodamine B. <b>2018</b> , 42, 2616-2626	9
308	Increased photocatalytic activity induced by TiO 2 /Pt/SnO 2 heterostructured films. <b>2018</b> , 76, 65-73	13
307	Ecofriendly Nanomaterials for Sustainable Photocatalytic Decontamination of Organics and Bacteria. <b>2018</b> , 1-29	О
306	SnO2/graphene quantum dots composited photocatalyst for efficient nitric oxide oxidation under visible light. <b>2018</b> , 448, 655-661	50
305	Novel diatom-FeOx composite as highly active catalyst in photodegradation of Rhodamine-6G. <b>2018</b> , 7, 247-255	9
304	Electrodeposition of CdSe/TiO2Coaxial Nanocables for Enhanced Photocatalytic Performance and H2Evolution in Visible Light. <b>2018</b> , 165, D160-D166	3
303	An eco-friendly highly stable and efficient Ni-C-S codoped wurtzite ZnO nanoplate: a smart photocatalyst for the quick removal of food dye under solar light irradiation. <b>2018</b> , 53, 2456-2467	3
302	Recent progress on the photocatalysis of carbon dots: Classification, mechanism and applications. <b>2018</b> , 19, 201-218	353

301	Anatase and rutile in evonik aeroxide P25: Heterojunctioned or individual nanoparticles?. <b>2018</b> , 300, 12-17	105
300	The role of graphene and europium on TiO2 performance for photocatalytic hydrogen evolution. <b>2018</b> , 44, 546-549	69
299	Dragon fruit-inspired quantum scale-designed photocathodes. <b>2018</b> , 213, 40-43	2
298	Synthesis of visible-light-driven BiOBrxI1-x solid solution nanoplates by ultrasound-assisted hydrolysis method with tunable bandgap and superior photocatalytic activity. <b>2018</b> , 732, 167-177	33
297	Hollow polydopamine colloidal composite particles: Structure tuning, functionalization and applications. <b>2018</b> , 513, 43-52	28
296	Conjugated microporous polymers bearing metallophthalocyanine moieties with enhanced visible-light photocatalytic activity. <b>2018</b> , 149, 261-267	16
295	Synthesis of Nanostructured Tin Oxide by Sol <b>©</b> el and Sonochemical Approaches in an Ionic Liquid. <b>2018</b> , 232, 245-256	6
294	Bridging Hydroxyls on Anatase TiO(101) by Water Dissociation in Oxygen Vacancies. <b>2018</b> , 122, 834-839	30
293	XANES study of vanadium and nitrogen dopants in photocatalytic TiO thin films. 2017, 20, 221-231	6
292	Polyol asserted hydrothermal synthesis of SnO2 nanoparticles for the fast adsorption and photocatalytic degradation of methylene blue cationic dye. <b>2018</b> , 42, 943-954	41
291	Two-Dimensional Transition Metal Oxide and Chalcogenide-Based Photocatalysts. <b>2018</b> , 10, 23	182
290	Enhanced photocatalytic activity and mechanism insight of MnOx/MIL-101. <b>2018</b> , 82, 226-232	10
289	Carbon quantum dots/KNbO3 hybrid composites with enhanced visible-light driven photocatalytic activity toward dye waste-water degradation and hydrogen production. <b>2018</b> , 445, 1-11	55
288	Silver Doped Niobium Pentoxide nanostructured thin film, Optical Structural and Morphological Properties. <b>2018</b> , 454, 012174	25
287	Preparation of Heteroleptic Tin(IV) N,O-Heteroarylalkenolate Complexes and Their Properties as PI-MOCVD Precursors for SnO2 Deposition. <b>2018</b> , 2018, 5027-5035	2
286	Review on design and evaluation of environmental photocatalysts. <b>2018</b> , 12, 1	131
285	Intrinsic AuPt-alloy particles decorated on TiO2 nanotubes provide enhanced photocatalytic degradation. <b>2018</b> , 292, 865-870	17
284	Dual-Functional Photocatalytic and Photoelectrocatalytic Systems for Energy- and Resource-Recovering Water Treatment. <i>ACS Catalysis</i> , <b>2018</b> , 8, 11542-11563	90

# (2018-2018)

283	Significantly Enhanced Aqueous Cr(VI) Removal Performance of Bi/ZnO Nanocomposites via Synergistic Effect of Adsorption and SPR-Promoted Visible Light Photoreduction. <b>2018</b> , 8, 426	15
282	Structural, morphological, optical and third order nonlinear optical response of spin-coated NiO thin films: An effect of N doping. <b>2018</b> , 86, 98-106	29
281	Tunable Transformation Between SnS and SnOx Nanostructures via Facile Anodization and Their Photoelectrochemical and Photocatalytic Performance. <b>2018</b> , 2, 1800161	7
280	Ultrathin nanosheets of graphitic carbon nitride heterojunction with flower like Bi2O3 for photodegradation of organic pollutants. <b>2018</b> , 5, 055030	1
279	Significant enhancement in photocatalytic performance of Ni doped BiFeO3 nanoparticles. 2018, 5, 065506	21
278	Photodegradation of organic dyes and industrial wastewater in the presence of layer-type perovskite materials under visible light irradiation. <b>2018</b> , 6, 4504-4513	17
277	Redox shuttle enhances nonthermal femtosecond two-photon self-doping of rGOIIiO2II photocatalysts under visible light. <b>2018</b> , 6, 16430-16438	20
276	Enhancement of photoelectrochemical performance of CdSe sensitized seeded TiO2 films. <b>2018</b> , 29, 16259-16269	5
275	Nanostructured mesoporous NiO as an efficient photocatalyst for degradation of methylene blue: Structure, properties and performance. <b>2018</b> , 16, 266-275	17
274	Recent Progress on Titanium Dioxide Nanomaterials for Photocatalytic Applications. 2018, 11, 3023-3047	158
274	Recent Progress on Titanium Dioxide Nanomaterials for Photocatalytic Applications. <b>2018</b> , 11, 3023-3047  Enhanced photocatalytic activity of Ag3PO4 via Fullerene C60 modification. <b>2018</b> , 32, e4472	158
273	Enhanced photocatalytic activity of Ag3PO4 via Fullerene C60 modification. <b>2018</b> , 32, e4472  Filling foaming agent into stacked layers: Rapid synthesis of graphitic carbon nitride nanosheets decorated with ultrafined MXY (X = O, S) nanoparticles for enhanced photoresponsive abilities.	1
273 272	Enhanced photocatalytic activity of Ag3PO4 via Fullerene C60 modification. <b>2018</b> , 32, e4472  Filling foaming agent into stacked layers: Rapid synthesis of graphitic carbon nitride nanosheets decorated with ultrafined MXY (X = O, S) nanoparticles for enhanced photoresponsive abilities. <b>2018</b> , 826, 52-59	3
273 272 271	Enhanced photocatalytic activity of Ag3PO4 via Fullerene C60 modification. <b>2018</b> , 32, e4472  Filling foaming agent into stacked layers: Rapid synthesis of graphitic carbon nitride nanosheets decorated with ultrafined MXY (X = O, S) nanoparticles for enhanced photoresponsive abilities. <b>2018</b> , 826, 52-59  Visible-light photoelectrodegradation of diuron on WO nanostructures. <b>2018</b> , 226, 249-255	1 3 10
273 272 271 270	Enhanced photocatalytic activity of Ag3PO4 via Fullerene C60 modification. <b>2018</b> , 32, e4472  Filling foaming agent into stacked layers: Rapid synthesis of graphitic carbon nitride nanosheets decorated with ultrafined MXY (X = O, S) nanoparticles for enhanced photoresponsive abilities. <b>2018</b> , 826, 52-59  Visible-light photoelectrodegradation of diuron on WO nanostructures. <b>2018</b> , 226, 249-255  Synergy of TiO2/Na0.23TiO2 Heterojunction for Enhanced Photocatalysis. <b>2018</b> , 53, 1700153  Enhanced visible-light-driven photodegradation of Rh-6G by surface engineered Pd-V2O5	1 3 10 6
273 272 271 270 269	Enhanced photocatalytic activity of Ag3PO4 via Fullerene C60 modification. 2018, 32, e4472  Filling foaming agent into stacked layers: Rapid synthesis of graphitic carbon nitride nanosheets decorated with ultrafined MXY (X = O, S) nanoparticles for enhanced photoresponsive abilities. 2018, 826, 52-59  Visible-light photoelectrodegradation of diuron on WO nanostructures. 2018, 226, 249-255  Synergy of TiO2/Na0.23TiO2 Heterojunction for Enhanced Photocatalysis. 2018, 53, 1700153  Enhanced visible-light-driven photodegradation of Rh-6G by surface engineered Pd-V2O5 heterostructure nanorods. 2018, 6, 5320-5331  The effects of nanoporous Fe2O3 synthesized via mechano-thermal process on electrical and	1 3 10 6

265	Aerosol Spray Pyrolysis Synthesis of Porous Anatase TiO2 Microspheres with Tailored Photocatalytic Activity. <b>2019</b> , 32, 286-296	4
264	Photocatalytic Studies of Composite Ferrite Nanoparticles. <b>2019</b> , 64, 946-954	9
263	Facile synthesis of rGO@In2S3@UiO-66 ternary composite with enhanced visible-light photodegradation activity for methyl orange. <b>2019</b> , 384, 112025	24
262	One-step impregnation method to prepare direct Z-scheme LaCoO3/g-C3N4 heterojunction photocatalysts for phenol degradation under visible light. <b>2019</b> , 491, 432-442	46
261	In Situ Photoelectrochemical Chloride Activation Using a WO Electrode for Oxidative Treatment with Simultaneous H Evolution under Visible Light. <b>2019</b> , 53, 9926-9936	43
260	Highly Efficient and Selective Oxidation of Ethanol to Acetaldehyde by a Hybrid Photocatalyst Consisting of SnO Nanorod and Rutile TiO with Heteroepitaxial Junction. <b>2019</b> , 20, 2155-2161	21
259	CoSe2 Clusters as Efficient Co-Catalyst Modified CdS Nanorod for Enhance Visible Light Photocatalytic H2 Evolution. <b>2019</b> , 9, 616	5
258	Controlled Hydrothermal Synthesis of Bismuth Vanadate Nano-articulate Structures: Photooxidation of Methicillin Resistant Staphylococcus aureus and Organic Dyes. <b>2019</b> , 9, 468-480	1
257	Cd(II) Based Coordination Polymer Series: Fascinating Structures, Efficient Semiconductors, and Promising Nitro Aromatic Sensing. <b>2019</b> , 19, 6431-6447	34
256	Facile synthesis of nickel oxide nanoparticles for the degradation of Methylene blue and Rhodamine B dye: a comparative study. <b>2019</b> , 13, 1108-1118	28
255	Enhanced photocatalytic activity of ZnONiO nanocomposites synthesized through a facile sonochemical route. <b>2019</b> , 1, 1	11
254	Green synthesis of metal oxide nanostructures using naturally occurring compounds for energy, environmental, and bio-related applications. <b>2019</b> , 43, 15846-15856	41
253	Palygorskite/g-C3N4 conjunction for visible-light-driven degradation of tetracycline hydrochloride. <b>2019</b> , 30, 18159-18167	2
252	Layer-by-layer assembly for photoelectrochemical nanoarchitectonics. <b>2019</b> , 4, 65-77	21
251	Comparative Study of EPR and Optical Properties of CdS, TiO2 and CdS-TiO2 Nanocomposite. <b>2019</b> , 48, 1545-1552	9
250	TiO2 nanotube arrays modified with nanoparticles of platinum group metals (Pt, Pd, Ru): enhancement on photoelectrochemical performance. <b>2019</b> , 21, 1	12
249	Membrane technology coupled with electrochemical advanced oxidation processes for organic wastewater treatment: Recent advances and future prospects. <b>2019</b> , 376, 120909	73
248	Plasmon-Assisted Photothermal Catalysis of Low-Pressure CO2 Hydrogenation to Methanol over Pd/ZnO Catalyst. <b>2019</b> , 11, 1598-1601	33

247	Innovative visualization of the effects of crystal morphology on semiconductor photocatalysts. Tuning the Hīlkel polarity of the shape-tailoring agents: the case of Bi2WO6. <b>2019</b> , 21, 1267-1278	6
246	Surface Engineering of Defective Hematite Nanostructures Coupled by Graphene Sheets with Enhanced Photoelectrochemical Performance. <b>2019</b> , 7, 12750-12759	4
245	MIL-53(Fe) incorporated in the lamellar BiOBr: Promoting the visible-light catalytic capability on the degradation of rhodamine B and carbamazepine. <b>2019</b> , 374, 975-982	74
244	Post-treatment with ZnFe2O4 nanoparticles to improve photo-electrochemical performance of ZnO nanorods based photoelectrodes. <b>2019</b> , 200, 109975	12
243	Recent Advances in Carbonaceous Photocatalysts with Enhanced Photocatalytic Performances: A Mini Review. <b>2019</b> , 12,	57
242	Gas-Phase Photoelectrocatalysis for Breaking Down Nitric Oxide. <b>2019</b> , 53, 7145-7154	27
241	Photocatalytic activity of TiO2 nanoparticles: a theoretical aspect. <b>2019</b> , 7, 13833-13859	84
240	CdS nanoparticles alleviate photo-induced stress in Geobacter co-cultures. <b>2019</b> , 6, 1941-1949	5
239	Synthesis of carbonaceous solid acid magnetic catalyst from empty fruit bunch for esterification of palm fatty acid distillate (PFAD). <b>2019</b> , 195, 480-491	28
238	Structural, electronic and optical properties of La, C-codoped TiO2 investigated by first principle calculations. <b>2019</b> , 132, 121-129	7
237	Solvent-driven morphology-controlled synthesis of highly efficient long-life ZnO/graphene nanocomposite photocatalysts for the practical degradation of organic wastewater under solar light. <b>2019</b> , 486, 37-51	30
236	A review on remediation of harmful dyes through visible light-driven WO3 photocatalytic nanomaterials. <b>2019</b> , 16, 4975-4988	26
235	Two-step hydrothermal fabrication of Na0.23TiO2 nanofibers and enhanced photocatalysis after loaded with gold or silver determined by surface potentials. <b>2019</b> , 43, 4062-4073	4
234	Enhanced visible light photoelectrochemical performance of Bi2O3-TiO2/ITO thin films prepared by aqueous sol-gel. <b>2019</b> , 23, 1757-1765	2
233	Hot carriers in action: multimodal photocatalysis on Au@SnO core-shell nanoparticles. 2019, 11, 7324-7334	19
232	ZnO/Ag/AgWO photo-electrodes with plasmonic behavior for enhanced photoelectrochemical water oxidation <i>RSC Advances</i> , <b>2019</b> , 9, 8271-8279	19
231	Self-limited ion-exchange grown Bi6Fe2Ti3O18-BiOBr ferroelectric heterostructure and the enhanced photocatalytic oxygen evolution. <b>2019</b> , 479, 137-147	16
230	High-Energy Electron-Beam-Induced Evolution of Secondary Phase and Enhanced Photocatalytic Activity in Monoclinic BiEuWO6 Nanoparticles. <b>2019</b> , 123, 10881-10892	3

229	Significance of an anion effect in the selective oxidation of Ce3+ to Ce4+ over a porous WO3 photoanode. <b>2019</b> , 307, 369-374	5
228	Visible light photocatalytic performance of laser-modified TiO2/SnO2 powders decorated with SiC nanocrystals. <b>2019</b> , 45, 12449-12454	12
227	Comparison of visible light photocatalytic degradation of different pollutants by (Zn, Mg)xCu1-xBi2O4 nanoparticles. <b>2019</b> , 45, 8926-8939	16
226	Visible light-driven photoelectrocatalytic degradation of acid yellow 17 using Sn3O4 flower-like thin films supported on Ti substrate (Sn3O4/TiO2/Ti). <b>2019</b> , 376, 196-205	20
225	Advanced Reduction and OxidationReduction Processes for Water Treatment. 2019, 1-13	
224	Photocatalytic Dye Degradation Using Modified Titania. <b>2019</b> , 171-199	4
223	. 2019,	2
222	Boosting interfacial charge transfer and electricity generation for levofloxacin elimination in a self-driven bio-driven photoelectrocatalytic system. <b>2019</b> , 11, 22042-22053	10
221	Nanostructured Metallic Oxides for Water Remediation. <b>2019</b> , 91-119	1
220	Fabrication of Ordered and High-Performance Nanostructured Photoelectrocatalysts by Electrochemical Anodization: Influence of Hydrodynamic Conditions. <b>2019</b> ,	
219	Synthesis of 1D-Anisotropic Particles Consisting of TiO Nanorods and SnO with Heteroepitaxial Junctions and Self-Assembled 3D-Microspheres. <b>2019</b> , 35, 17096-17102	6
218	Graphene-based plasmonic nanocomposites for highly enhanced solar-driven photocatalytic activities <i>RSC Advances</i> , <b>2019</b> , 9, 30585-30598	8
217	Photoinduced electron transfer in semiconductor lay binary nanosheet colloids controlled by clay particles as a turnout switch. <b>2019</b> , 241, 499-505	9
216	Electrodeposition of WO3 on Ti substrate and the influence of interfacial oxide layer generated in situ: A photoelectrocatalytic degradation of propyl paraben. <b>2019</b> , 464, 664-672	27
215	Polydopamine-Inspired Design and Synthesis of Visible-Light-Driven Ag [email´protected]@elongated TiO2 NTs CoreBhell Nanocomposites for Sustainable Hydrogen Generation. <b>2019</b> , 7, 558-568	34
214	Surface and interface engineering of hierarchical photocatalysts. <b>2019</b> , 471, 43-87	135
213	Design of visible-light photocatalysts by coupling of inorganic semiconductors. <b>2019</b> , 335, 3-19	26
212	LaMnO3 nanoparticles supported on N doped porous carbon as efficient photocatalyst. <b>2019</b> , 159, 59-68	18

## (2020-2019)

211	Charge carrier trapping, recombination and transfer during TiO2 photocatalysis: An overview. <b>2019</b> , 335, 78-90	199
210	Improvement in the visible light mediated photocatalytic activity of Al2O3 nanoparticles through Zn2+ doping. <b>2019</b> , 17, 67-76	15
209	A review on greywater reuse: quality, risks, barriers and global scenarios. <b>2019</b> , 18, 77-99	33
208	Photocatalytic activity of Zr2(WO4)(PO4)2. <b>2019</b> , 45, 1430-1433	1
207	Preparation of lignin/TiO2 nanocomposites and their application in aqueous polyurethane coatings. <b>2019</b> , 13, 59-69	17
206	Enhanced photocatalytic activity of ZnO/g-CN composites by regulating stacked thickness of g-CN nanosheets. <b>2020</b> , 257, 113577	14
205	A Biotemplating Route for the Synthesis of Hierarchical Fe O with Highly Dispersed Carbon as Electron-Transfer Channel. <b>2020</b> , 85, 258-263	3
204	Hybrid polyoxometalates as post-functionalization platforms: from fundamentals to emerging applications. <b>2020</b> , 49, 382-432	133
203	In situ growth of M-{001}TiO/Ti photoelectrodes: synergetic dominant {001} facets and ratio-optimal surface junctions for the effective oxidation of environmental pollutants. <b>2020</b> , 56, 1337-1340	24
202	Coupled-substituted double-layer Aurivillius niobates: structures, magnetism and solar photocatalysis. <b>2020</b> , 49, 1433-1445	6
201	Photocatalysts for H Generation from Starburst Triphenylamine/Carbazole Donor-Based Metal-Free Dyes and Porous Anatase TiO Cube. <b>2020</b> , 13, 1037-1043	10
200	Synthesis and Photocatalytic Activity of WO3 Nanoparticles Prepared by Underwater Impulse Discharge. <b>2020</b> , 40, 571-587	13
199	Interface tailoring of SnO2IIiO2 photocatalysts modified with anionic/cationic surfactants. <b>2020</b> , 55, 3279-3298	4
198	Synthesis and characterisation of the mesoporous ZnO-TiO2 nanocomposite; Taguchi optimisation and photocatalytic methylene blue degradation under visible light. <b>2020</b> , 35, 281-289	13
197	A review on metal-organic frameworks for photoelectrocatalytic applications. 2020, 31, 1773-1781	22
196	Ultra-thin rGO nanosheet modified TiO2 nanotube arrays for boosted photoelectrochemical performance. <b>2020</b> , 506, 144966	20
195	An impact of La doping content on physical properties of NiO films facilely casted through spin-coater for optoelectronics. <b>2020</b> , 582, 411955	11
194	Action of chloride ions as a habit modifier in the hydrothermal crystal growth of rutile TiO2 nanorod from SnO2 seed crystal. <b>2020</b> , 761, 138003	3

193	CuO-NiO-TiO2 bimetallic nanocomposites for catalytic applications. <b>2020</b> , 496, 111193	2
192	Nanohybrid Crystals with Heteroepitaxial Junctions for Solar-to-Chemical Transformations. <b>2020</b> , 124, 25657-25666	5
191	Innovative and Cost-Efficient BiOI Immobilization Technique on Ceramic Paper-Total Coverage and High Photocatalytic Activity. <b>2020</b> , 10,	8
190	Ultrafast Charge Carrier Dynamics in Vanadium-Modified TiO2 Thin Films and Its Relation to Their Photoelectrocatalytic Efficiency for Water Splitting. <b>2020</b> , 124, 26572-26582	3
189	Optical and photocatalytic properties of ZnO and ZnS structures formed as controlled calcination products of l-cysteine assisted aqueous precipitation. <b>2020</b> , 25, 101573	1
188	Rapid and Low-Temperature Molecular Precursor Approach toward Ternary Layered Metal Chalcogenides and Oxides: Mo W S and Mo W O Alloys (0 🔟). <b>2020</b> , 32, 7895-7907	7
187	Evaluating the Effect of WO3 on Electrochemical and Corrosion Properties of TiO2-RuO2-Coated Titanium Anodes with Low Content of RuO2. <b>2020</b> , 11, 555-566	8
186	Anomalous Charge Carrier Decay Spotted by Clustering of a Time-Resolved Microscopic Phase Image Sequence. <b>2020</b> , 124, 23551-23557	6
185	Enhanced CO Sensing Performances of PdO/WO Determined by Heterojunction Structure under Illumination. <b>2020</b> , 5, 28784-28792	3
184	Photo-electrochemical degradation of wastewaters containing organics catalysed by phosphate-based materials: a review. <b>2020</b> , 19, 843-872	14
183	Liquid-Phase Exfoliated GeSe Nanoflakes for Photoelectrochemical-Type Photodetectors and Photoelectrochemical Water Splitting. <b>2020</b> , 12, 48598-48613	21
182	Synthesis of Core-Shell Au@TiO2@C Nanoparticles and Their Photocatalytic Properties for the Degradation of Rhodamine B Under Simulated-Solar Light. <b>2020</b> , 5, 10055-10059	O
181	Dynamics of Photogenerated Charge Carriers in TiO2/MoO3, TiO2/WO3 and TiO2/V2O5 Photocatalysts with Mosaic Structure. <b>2020</b> , 10, 1022	5
180	Photocatalytic H Production from Water by Metal-free Dye-sensitized TiO Semiconductors: The Role and Development Process of Organic Sensitizers. <b>2020</b> , 13, 5863-5895	20
179	Photodegradation of methylene blue under UV and visible light irradiation by Er2O3-coated silicon nanowires as photocatalyst. <b>2020</b> , 131, 525-536	O
178	Enhanced Photocatalytic Performance of Nanosized Mixed-Ligand Metal-Organic Frameworks through Sequential Energy and Electron Transfer Process. <b>2020</b> , 59, 12947-12953	14
177	A Selective Synthesis of TaON Nanoparticles and Their Comparative Study of Photoelectrochemical Properties. <b>2020</b> , 10, 1128	3
176	Surface Chemistry of Gallium-Based Liquid Metals. <b>2020</b> , 3, 1477-1506	34

## (2020-2020)

175	Ti-MOF Derived N-Doped TiO2 Nanostructure as Visible-light-driven Photocatalyst. <b>2020</b> , 36, 447-452	13
174	Promoted photoelectrocatalytic degradation of BPA with peroxymonosulfate on a MnFe2O4 modified carbon paper cathode. <b>2020</b> , 399, 125088	27
173	Optical properties of W1MMoxO3?0.33H2O semiconductor oxides synthesized by hydrothermal and microwave techniques. <b>2020</b> , 119, 107984	
172	InGaN Nanorods Decorated with Au Nanoparticles for Enhanced Water Splitting Based on Surface Plasmon Resonance Effects. <b>2020</b> , 10,	5
171	Semiconductor Electrode Materials Applied in Photoelectrocatalytic Wastewater Treatment Overview. <b>2020</b> , 10, 439	30
170	Fabrication and photoelectrocatalytic performance of C3N4-modified Ti/PbO2 anode with surface hydrophobicity. <b>2020</b> , 24, 1577-1585	3
169	Synthesis and high photocatalytic performance of a novel hollow meso-TiO2/ZnO composite microsphere. <b>2020</b> , 95, 344-352	2
168	Enhanced Electrochromic Properties by Improvement of Crystallinity for Sputtered WO3 Film. <b>2020</b> , 10, 577	12
167	Plasmon-induced photocatalytic transformations. <b>2020</b> , 249-275	
166	Photocatalytic degradation of penicillin G from simulated wastewater using the UV/ZnO process: isotherm and kinetic study. <b>2020</b> , 18, 107-117	18
165	Advanced materials for photocatalytic applications: the challenge ahead. 2020, 3-8	3
164	Photoelectrocatalytic degradation of Rhodamine B using N doped TiO2 thin Films. <b>2020</b> , 23, 382-388	5
163	Tetracycline Photocatalytic Degradation under CdS Treatment. <b>2020</b> , 8, 483	16
162	Modified Nano-TiO2 Based Composites for Environmental Photocatalytic Applications. <b>2020</b> , 10, 759	16
161	A photoactive process cascaded electrocatalysis for enhanced methanol oxidation over Pt-MXene-TiO2 composite. <b>2020</b> , 13, 2683-2690	17
160	The roles of graphene and sandwich structure in rGO/BiOI/rGO to enhance the photoelectrocatalytic activity. <b>2020</b> , 289, 121480	6
159	Microstructure, optical and photocatalytic properties of MgO nanoparticles. 2020, 16, 103013	38
158	Visible light active heterostructured photocatalyst system based on CuO plate-like particles and SnO2 nanofibers. <b>2020</b> , 17, 1479-1489	12

157	Fabrication of BiOCl/ZnO/CN Nanocomposite for Visible-Light Photocatalytic Degradation of Dyes. <b>2020</b> , 5, 1640-1647		6
156	Design of an alkaline pyridyl acceptor-based calix[4]arene dye and synthesis of stable calixarene <b>T</b> iO2 porous hybrid materials for efficient photocatalysis. <b>2020</b> , 8, 8883-8891		12
155	Highly efficient visible light driven photocatalytic activity of graphene and CNTs based Mg doped ZnO photocatalysts: A comparative study. <b>2020</b> , 245, 116892		14
154	A novel zero valent metal bismuth for bromate removal: direct and ultraviolet enhanced reduction <i>RSC Advances</i> , <b>2020</b> , 10, 4148-4155	3.7	3
153	Principle and surface science of photocatalysis. <b>2020</b> , 31, 1-38		7
152	Metal-oxide semiconductor photocatalysts for the degradation of organic contaminants. <b>2020</b> , 23-38		1
151	Nanosheets-assembled Bi2WO6 microspheres with efficient visible-light-driven photocatalytic activities. <b>2020</b> , 163, 110297		18
150	Structurally and Compositionally Tunable Absorption Properties of AgCl@AgAu Nanocatalysts for Plasmonic Photocatalytic Degradation of Environmental Pollutants. <b>2020</b> , 10, 405		2
149	Defect-Induced Acceleration and Deceleration of Photocarrier Recombination in SrTiO3 Powders. <b>2020</b> , 124, 11057-11063		9
148	Hybridized 2D Nanomaterials Toward Highly Efficient Photocatalysis for Degrading Pollutants: Current Status and Future Perspectives. <b>2020</b> , 16, e1907087		41
147	Efficient Photodegradation of Rhodamine B and Tetracycline over Robust and Green g-CN Nanostructures: Supramolecular Design. <b>2021</b> , 403, 123703		35
146	Covalent organic framework nanorods bearing single Cu sites for efficient photocatalysis. <b>2021</b> , 403, 126383		34
145	CuxNi1-xO nanostructures and their nanocomposites with reduced graphene oxide: Synthesis, characterization, and photocatalytic applications. <b>2021</b> , 47, 3603-3613		47
144	Microwave-assisted synthesis of various Cu2O/Cu/TiO2 and CuxS/TiO2 composite nanoparticles towards visible-light photocatalytic applications. <b>2021</b> , 259, 123986		2
143	A comprehensive review on catalysts for electrocatalytic and photoelectrocatalytic degradation of antibiotics. <b>2021</b> , 409, 127739		40
142	Recent Advance in Carbon Dots: From Properties to Applications. <b>2021</b> , 39, 1364-1388		7
141	Enhanced fenton-like catalysis by facilely prepared nano-scale NCFOH/HKUST composites with synergistic effect for dye degradation. <b>2021</b> , 258, 123980		3
140	Evaluation of the sono-assisted photolysis method for the mineralization of toxic pollutants. <b>2021</b> , 258, 117903		10

139	Photocatalytic degradation of dyes using phosphorus-containing activated carbons. 2021, 535, 147667	6
138	Interfacial Charge Transport in 1D TiO Based Photoelectrodes for Photoelectrochemical Water Splitting. <b>2021</b> , 17, e1903378	48
137	Modulating Photoinduced Charge Separation in Metal Zolate Frameworks. 2021, 125, 2064-2073	1
136	Semiconductor @ sensitizer composites for enhanced photoinduced processes. <b>2021</b> , 183-209	O
135	Silver nanoparticle-decorated titanium dioxide nanowire systems bioinspired poly(L-DOPA) thin film as a surface-enhanced Raman spectroscopy (SERS) platform, and photocatalyst. <b>2021</b> , 23, 13396-13404	4
134	Cation disorder and octahedral distortion control of internal electric field, band bending and carrier lifetime in Aurivillius perovskite solid solutions for enhanced photocatalytic activity.	4
133	Enhanced photocatalytic activity, transport properties and electronic structure of Mn doped GdFeO synthesized using the sol-gel process. <b>2021</b> , 23, 16060-16076	6
132	Application of polyoxometalates in photocatalytic degradation of organic pollutants. <b>2021</b> , 3, 4646-4658	12
131	Plant-Based Natural Dye-Stimulated Visible-Light Reduction of GO and Physicochemical Factors Influencing the Production of Oxidizing Species by a Synthesized (rGO)/TiO Nanocomposite for Environmental Remediation. <b>2021</b> , 6, 2686-2698	2
130	Chalcogenides as well as chalcogenides-based nanomaterials and its importance in photocatalysis. <b>2021</b> , 33-76	O
129	An overview: recent development of semiconductor/graphene nanocomposites for photodegradation of phenol and phenolic compounds in aqueous solution. <b>2021</b> , 9, 1-23	4
128	ZnO nanorods/FeO-graphene oxide/metal-organic framework nanocomposite: recyclable and robust photocatalyst for degradation of pharmaceutical pollutants. <b>2021</b> , 28, 21799-21811	3
127	Basic principles, fundamentals, and mechanisms of chalcogenide-based nanomaterials in photocatalytic reactions. <b>2021</b> , 77-103	1
126	Photocatalytic Hydrogen Evolution Over Pt/Co-TiO2 Photocatalysts. <b>2021</b> , 2, 35-48	
125	Synthesis and electrochemical characterization of Si/TiO2/Au composite anode: Efficient oxygen evolution and hydroxyl radicals generation. <b>2021</b> , 370, 137742	3
124	Photoaccumulating Nanoheterostructures Based on Titanium Dioxide. <b>2021</b> , 55, 219-227	2
123	Photoelectrochemical performance of MWCNTAgInO ternary hybrid: a study of Ag loading and MWCNT garnishing. <b>2021</b> , 56, 8627-8642	3
122	Structural, Optical and Dielectric Properties of Nd Doped NiO Thin Films Deposited with a Spray Pyrolysis Method. <b>2021</b> , 31, 2691-2699	4

121	Atomic Level Interface Control of SnO2-TiO2 Nanohybrids for the Photocatalytic Activity Enhancement. <b>2021</b> , 11, 205	3
120	Intensification of Heterogeneous Photocatalytic Reactions Without Efficiency Losses: The Importance of Surface Catalysis. <b>2021</b> , 151, 3105-3113	5
119	Impact of humidity on the removal of volatile organic compounds over Fe loaded TiO2 under visible light irradiation: Insight into photocatalysis mechanism by operando DRIFTS. <b>2021</b> , 26, 102119	4
118	Tailoring the Optical Properties of Sputter-Deposited Gold Nanostructures on Nanostructured Titanium Dioxide Templates Based on Grazing-Incidence Small-Angle X-ray Scattering Determined Growth Laws. <b>2021</b> , 13, 14728-14740	2
117	Preparation and application of defective graphite phase carbon nitride photocatalysts. 2021,	
116	Facile synthesis of cooperative mesoporous-assembled CexSr1-xFexTi1-xO3 perovskite catalysts for enhancement beta-lactam antibiotic photodegradation under visible light irradiation. <b>2021</b> , 23, 101013	2
115	Low Temperature Aqueous Chemical Growth Method for the Doping of W into ZnO Nanostructures and Their Photocatalytic Role in the Degradration of Methylene Blue. 1	2
114	Operando Raman and UV-Vis spectroscopic investigation of the coloring and bleaching mechanism of self-powered photochromic devices for smart windows. <b>2021</b> , 82, 105721	7
113	Photocatalytic Technology for Palm Oil Mill Effluent (POME) Wastewater Treatment: Current Progress and Future Perspective. <b>2021</b> , 14,	6
112	Photocatalytic organic dye by two new coordination polymers with flexible dicarboxylate and different N-donor linkage. <b>2021</b> , 519, 120284	2
111	Photoelectrochemical Cytosensors.	0
110	Green and Cost-Effective Synthesis of Tin Oxide Nanoparticles: A Review on the Synthesis Methodologies, Mechanism of Formation, and Their Potential Applications. <b>2021</b> , 16, 97	11
109	Boosting of photocatalytic hydrogen evolution via chlorine doping of polymeric carbon nitride. <b>2021</b> , 12, 473-484	2
108	Synthesis of metal-free phosphorus doped graphitic carbon nitride-P25 (TiO2) composite: Characterization, cyclic voltammetry and photocatalytic hydrogen evolution. <b>2021</b> , 223, 110958	9
107	Carboxylate Adsorption on Rutile TiO(100): Role of Coulomb Repulsion, Relaxation, and Steric Hindrance. <b>2021</b> , 125, 13770-13779	3
106	Improved UV Photodetection of Terbium-doped NiO thin films prepared by cost-effective nebulizer spray technique. <b>2021</b> , 127, 105673	8
105	Photo-electrochemical Production of IO4lfrom IO3lbver a WO3 Semiconductor Photoanode. <b>2021</b> , 50, 1220-1222	1
104	Recent advancements of spinel ferrite based binary nanocomposite photocatalysts in wastewater treatment. <b>2021</b> , 274, 129734	30

103	Construction of an arsenene/g-C3N4 hybrid heterostructure towards enhancing photocatalytic activity of overall water splitting: A first-principles study. <b>2021</b> , 299, 122138	3
102	Magnetic Field-Assisted Photocatalytic Degradation of Organic Pollutants over BiRFeO (R = Ce, Tb; $x = 0.00, 0.05, 0.10$ and 0.15) Nanostructures. <b>2021</b> , 14,	O
101	Novel AgClxBr1⊠ solid solutions photocatalyst with enhanced photocatalytic activity for reduction of Cr6+ and oxidation of Bisphenol A under simulated sunlight. <b>2021</b> , 139, 111257	1
100	Reduced graphene oxide-ZnO hybrid composites as photocatalysts: The role of nature of the molecular target in catalytic performance. <b>2021</b> , 47, 19346-19355	2
99	Photocatalyst-enzyme hybrid systems for light-driven biotransformation. <b>2021</b> , 54, 107808	2
98	Photocatalytic NOx removal using tantalum oxide nanoparticles: A benign pathway. <b>2021</b> , 291, 119974	20
97	A Review on Metal Ions Modified TiO2 for Photocatalytic Degradation of Organic Pollutants. <b>2021</b> , 11, 1039	12
96	Solar-Driven Photoelectrochemical Performance of Novel ZnO/AgWO/AgBr Nanorods-Based Photoelectrodes. <b>2021</b> , 16, 133	1
95	Shedding Light on the Role of Chemical Bond in Catalysis of Nitrogen Fixation. 2021, 33, e2007891	6
94	Synthesis of WO3 nanorods through anodization in the presence of citric acid: Formation mechanism, properties and photoelectrocatalytic performance. <b>2021</b> , 422, 127489	3
93	Polymer Nanocomposite Films Based on Two-Dimensional Materials for Photocatalytic Applications. <b>2022</b> , 111-143	1
92	Enhanced singlet oxygen photogeneration by bactericidal ZnOMgOAg nanocomposites. <b>2021</b> , 276, 125204	2
91	Constructed Co3O4-Sn3O4 hierarchical nanoflower-tree heterostructure with boosting photoelectrocatalytic efficiency for water decontamination. <b>2021</b> , 423, 130252	7
90	Development of a three-dimensional photoelectrocatalytic reactor packed with granular sludge carbon photoelectrocatalyst for efficient wastewater treatment. <b>2021</b> , 277, 119642	O
89	CQDs/biochar from reed straw modified Z-scheme MgInS/BiOCl with enhanced visible-light photocatalytic performance for carbamazepine degradation in water. <b>2022</b> , 287, 132192	9
88	Transition metal chalcogenideBased photocatalysts for small-molecule activation. <b>2021</b> , 297-331	1
87	Heterojunctions: Joining Different Semiconductors. 2013, 311-327	1
86	Photo-Catalytic Hydrogen Production. <b>2012</b> , 1099-1121	3

85	Electrochemistry: A Powerful Tool for Preparation of Semiconductor Materials for Decontamination of Organic and Inorganic Pollutants, Disinfection, and CO2 Reduction. <b>2017</b> , 239-269	1
84	Electrospun Nanofiber-Based Photocatalysts. <b>2014</b> , 371-401	1
83	Heat treatment effect of a hybrid consisting of SnO2 nanorod and rutile TiO2 with heteroepitaxial junction on the photocatalytic activity. <b>2020</b> , 147, 106148	4
82	Efficient photodecomposition of herbicide imazapyr over mesoporous GaO-TiO nanocomposites. <b>2018</b> , 342, 519-526	37
81	Low-cost microbiological purification using a new ceramic disk filter functionalized by chitosan/TiO2 nanocomposites. <b>2020</b> , 248, 116984	11
80	Effect of surface modification and H2 reduction of WO3 nanoparticles in Methylene Blue photodegradation. <b>2020</b> , 8, 045012	1
79	Photocatalytic properties for different metal-oxide nanomaterials. 2019,	1
78	Electrically switchable photonic crystals based on liquid-crystal-infiltrated TiO-inverse opals. <b>2019</b> , 27, 15391-15398	7
77	Efficient visible light photocatalysis of benzene, toluene, ethylbenzene and xylene (BTEX) in aqueous solutions using supported zinc oxide nanorods. <b>2017</b> , 12, e0189276	24
76	LaCo xFe 1-XO 3 (.	
76 75	LaCo xFe 1-XO 3 (.  Di-functional Cu-doped BiOCl photocatalyst for degradation of organic pollutant and inhibition of cyanobacterial growth. 2021, 424, 127554	2
•	Di-functional Cu-doped BiOCl photocatalyst for degradation of organic pollutant and inhibition of	2
75	Di-functional Cu-doped BiOCl photocatalyst for degradation of organic pollutant and inhibition of cyanobacterial growth. <b>2021</b> , 424, 127554	
75 74	Di-functional Cu-doped BiOCl photocatalyst for degradation of organic pollutant and inhibition of cyanobacterial growth. 2021, 424, 127554  A review of nanotechnological applications to detect and control surface water pollution. 2021, 24, 102032  Photoelectrocatalytic coupling system synergistically removal of antibiotics and antibiotic resistant	10
75 74 73	Di-functional Cu-doped BiOCl photocatalyst for degradation of organic pollutant and inhibition of cyanobacterial growth. 2021, 424, 127554  A review of nanotechnological applications to detect and control surface water pollution. 2021, 24, 102032  Photoelectrocatalytic coupling system synergistically removal of antibiotics and antibiotic resistant bacteria from aquatic environment. 2021, 424, 127553  Photoelectrochemical properties of WO3-modified anatase TiO2 photoanodes and application for	10
75 74 73 72	Di-functional Cu-doped BiOCl photocatalyst for degradation of organic pollutant and inhibition of cyanobacterial growth. 2021, 424, 127554  A review of nanotechnological applications to detect and control surface water pollution. 2021, 24, 102032  Photoelectrocatalytic coupling system synergistically removal of antibiotics and antibiotic resistant bacteria from aquatic environment. 2021, 424, 127553  Photoelectrochemical properties of WO3-modified anatase TiO2 photoanodes and application for dye-sensitized solar cells. 2021, 27, 101543	10
75 74 73 72 71	Di-functional Cu-doped BiOCl photocatalyst for degradation of organic pollutant and inhibition of cyanobacterial growth. 2021, 424, 127554  A review of nanotechnological applications to detect and control surface water pollution. 2021, 24, 102032  Photoelectrocatalytic coupling system synergistically removal of antibiotics and antibiotic resistant bacteria from aquatic environment. 2021, 424, 127553  Photoelectrochemical properties of WO3-modified anatase TiO2 photoanodes and application for dye-sensitized solar cells. 2021, 27, 101543  Encyclopedia of Sustainability Science and Technology. 2012, 7881-7901	10

67	Sonochemical Synthesis of Zinc Sulfide Photocatalysts and Their Environmental Applications. <b>2015</b> , 1-33	
66	The Effects of WO3Nanoparticles Addition to the TiO2Photoelectrode in Dye-Sensitized Solar Cells. <b>2016</b> , 4, 42-47	2
65	Ecofriendly Nanomaterials for Sustainable Photocatalytic Decontamination of Organics and Bacteria. <b>2019</b> , 1777-1805	
64	Synthesis and Characterization of Single-Phased BiFeO3 Nanostructures for Photocatalytic Applications: Hydrothermal Approach. <b>2020</b> , 295-315	
63	EFFECT OF SUNLIGHT ON THE ELECTRICAL CHARACTERISTICS OF THE HETEROSTRUCTURE TITANIUM DIOXIDE/SILICON. <b>2019</b> , 136-143	
62	The Use of a Novel Three-Electrode Impulse Underwater Discharge for the Synthesis of W-Mo Mixed Oxide Nanocomposites. 1	1
61	Unraveling Electron-deficient Setaria-viridis-like Co3O4@MnO2 heterostructure with superior photoelectrocatalytic efficiency for water remediation. <b>2022</b> , 573, 151473	3
60	TiO2/SnO2 nano-composite: New insights in synthetic, structural, optical and photocatalytic aspects. <b>2022</b> , 529, 120640	5
59	Effect of Bi doping on the structural and optical properties of NiO thin films. 2022, 146, 107579	0
58	Metal Oxide-Based Nanocomposites Application Towards Photocatalysis. <b>2020</b> , 155-178	
57	LaCoFeO (OMI) spherical nanostructures prepared via ultrasonic approach as photocatalysts. <b>2021</b> , 80, 105824	0
56	Enhanced photocatalytic hydrogen production by loading histidine on TiO2. <b>2021</b> , 3, 014001	O
55	BiOCl microspheres with controllable oxygen vacancies: Synthesis and their enhanced photocatalytic performance. <b>2021</b> , 306, 122751	2
54	Effect of the Type of Heterostructures on Photostimulated Alteration of the Surface Hydrophilicity: TiO2/BiVO4 vs. ZnO/BiVO4 Planar Heterostructured Coatings. <b>2021</b> , 11, 1424	2
53	Advances in photoelectroreduction of CO2 to hydrocarbons fuels: Contributions of functional materials. <b>2021</b> , 55, 101810	4
52	Air Purification Using Polymer Fiber Filters. 2100753	3
51	Photoelectrocatalytic Solar Water Splitting. <b>2022</b> , 241-274	
50	Electrospun Nanocomposite Materials for Environmental and Energy Applications. 2022, 221-249	

49	Template-directed synthesis of pomegranate-shaped zinc oxide@zeolitic imidazolate framework for visible light photocatalytic degradation of tetracycline <b>2022</b> , 294, 133782		O
48	Photocatalytic Aspect of Rgo/Mnfe2o4 as an Efficient Magnetically Retrievable Catalyst for Reduction of Nitroaromatic Compounds Under Visible-Light Irradiation.		
47	Coexisting Chloride Ion for Boosting the Photoelectrocatalytic Degradation Efficiency of Organic Dyes. 1		
46	Layered Ti-based oxide hierarchical nanocomposites derived from flash oxidation of MXene with enhanced photocatalytic and microwave transparent performance. <b>2022</b> ,		2
45	Cobalt-doped UiO-66 nanoparticle as a photo-assisted Fenton-like catalyst for the degradation of rhodamine B. <b>2022</b> , 643, 128734		1
44	Wavelength Dependence of the Transformation Mechanism of Sulfonamides Using Different LED Light Sources and TiO and ZnO Photocatalysts <b>2021</b> , 15,		2
43	Robust Photoelectrochemical Route for the Ambient Fixation of Dinitrogen into Ammonia over a Nanojunction Assembled from Ceria and an Iron Boride/Phosphide Cocatalyst <b>2021</b> ,		2
42	Synthesis of Sn and Zr-Doped BiVO 4 Nanocatalyst with Enhanced Photocatalytic and Photoelectrochemical Activity. <b>2022</b> , 7,		O
41	Heterostructured MXene-derived oxides as superior photocatalysts for MB degradation. <b>2022</b> , 165629		0
40	Influence of mass ratio and calcination temperature on physical and photoelectrochemical properties of ZnFe-layered double oxide/cobalt oxide heterojunction semiconductor for dye degradation applications. <i>Particuology</i> , <b>2022</b> ,	2.8	5
39	WO3-based materials as heterogeneous catalysts for diverse organic transformations: a mini-review. <i>Synthetic Communications</i> , 1-20	1.7	0
38	Photocatalytic dye-degradation activity of nano-crystalline Ti1 $\mathbb{N}$ MxO2 $\mathbb{I}$ M =Ag, Pd, Fe, Ni and x = 0, 0.01) for water pollution abatement. <i>RSC Advances</i> , <b>2022</b> , 12, 18794-18805	3.7	O
37	Subtle Structure Matters: The Vicinity of Surface Ti5c Cations Alters the Photooxidation Behaviors of Anatase and Rutile TiO2 under Aqueous Environments. <i>ACS Catalysis</i> , <b>2022</b> , 12, 8242-8251	13.1	0
36	Identifying Photocatalytic Active Sites of C2H6 CH Bond Activation on TiO2 via Combining First-Principles Ground-State and Excited-State Electronic Structure Calculations. <i>Journal of Physical Chemistry Letters</i> , 6532-6540	6.4	1
35	Achieving over 18 % Efficiency Organic Solar Cell Enabled by a ZnO-Based Hybrid Electron Transport Layer with an Operational Lifetime up to 5 Years. <i>Angewandte Chemie - International Edition</i> ,	16.4	5
34	Recent Advances in Aerobic Photo-Oxidation over Small-Sized IB Metal Nanoparticles. <i>Photochem</i> , <b>2022</b> , 2, 528-538		O
33	Achieving over 18 % Efficiency Organic Solar Cell Enabled by a ZnO-Based Hybrid Electron Transport Layer with an Operational Lifetime up to 5 Years. <i>Angewandte Chemie</i> ,	3.6	0
32	H 2 O 2 assisted photocatalysis over Fe-MOF modified BiOBr for degradation of RhB. <i>Journal of Chemical Technology and Biotechnology</i> ,	3.5	2

31	Machine learning ensures rapid and precise selection of gold sea-urchin-like nanoparticles for desired light-to-plasmon resonance.	O
30	Template-free synthesis of novel TiO2 microtube (MT) and N-doped MT and their photocatalytic properties decomposing organic compounds. <b>2022</b> , 118841	O
29	Photocatalytic aspect of rGO/MnFe2O4 as an efficient magnetically retrievable catalyst for reduction of nitroaromatic compounds under visible-light irradiation. <b>2022</b> , 10, 108368	0
28	Nanohybrid Photocatalysts with Heteroepitaxial Junction for Solar Chemical Transformations. <b>2022</b> , 95, 275-281	O
27	Photoelectrocatalytic systems for simultaneous energy recovery and wastewater treatment: a review.	0
26	Aligning Fe2O3 photo-sheets on TiO2 nanofibers with hydrophilic and aerophobic surface for boosting photoelectrochemical performance.	Ο
25	Photodegradation of Rhodamine B and Crystal Violet using Al-doped CoMn nanoferrites and dielectric study.	1
24	Novel Bi2Sn2O7 quantum dots/TiO2 nanotube arrays S-scheme heterojunction for enhanced photoelectrocatalytic degradation of sulfamethazine. <b>2022</b> , 122053	2
23	Atomistic Insights of Ti-Based MXenes Thermal Decomposition and Transformation to Carbon-Supported Ti <b>D</b> Phases for Energy Applications.	0
22	Ag3PO4 and Ag3PO4Based visible light active photocatalysts: Recent progress, synthesis, and photocatalytic applications. <b>2022</b> , 106556	2
21	Photocatalytic properties of two new isostructural cobalt(II) and nickel(II) complexes having terphenyl-3,3?,4,4?-teteacarboxylic acid. <b>2022</b> , 228, 116158	0
20	Preparation and photocatalytic property of exfoliated poly(phenylenethiazolo[5,4-d]thiazole) copolymers.	O
19	Electrospun Bi-decorated BixTiyOz/TiO2 flexible carbon nanofibers and their applications on degradating of organic pollutants under solar radiation. <b>2022</b> ,	8
18	Nitrogen-doped carbon dots as visible light initiators for 3D (bio)printing.	O
17	A novel nitrogenous core-shell MIL-101(Fe)-based nanocomposite for enhanced adsorption and photo-degradation of organic pollutant under visible light. <b>2023</b> , 938, 168479	0
16	Synthesis and Photocatalytic Applications of Functionalized Carbon Quantum Dots. <b>2022</b> , 95, 1638-1679	2
15	Hotspots and Tendencies of Energy Optimization Based on Bibliometric Review. 2023, 16, 158	0
14	Development of Bi2WO6 and Bi2O3 IZnO heterostructure for enhanced photocatalytic mineralization of Bisphenol A.	O

13	Engineering of graphitic carbon nitride-based heterojunction photocatalysts. 2023, 43-57	О
12	Chemical reduction of porous WO3 and TiO2 photoelectrocatalysts by atomic hydrogen. <b>2023</b> , 658, 119163	O
11	Red anatase TiO2 microspheres with exposed major {0 0 1} facets and boron-stabilized hydrogen-occupied oxygen vacancies for visible-light-responsive water oxidation. <b>2023</b> , 640, 211-219	0
10	Strategic growth engineering of Ag self-doped Ag2CO3 on MIL-53 MOF: A novel p-n heterostructure facilitates serendipitous charge migration and remarkable multimodal photocatalytic activity. <b>2023</b> , 35, 105842	O
9	Comparative study of TiO2 and palladium doped TiO2 nano catalysts for water purification under solar and ultraviolet irradiation. <b>2023</b> , 1, 100002	О
8	Photoreforming of Waste Polymers for Sustainable Hydrogen Fuel and Chemicals Feedstock: Waste to Energy.	О
7	Dual doping effect of Ag+ & amp; Al3+ on the structural, optical, photocatalytic properties of ZnO nanoparticles. <b>2023</b> , 13, 100382	О
6	Low-temperature synthesis one-dimensional Ag 2 CO 3 /SnFe 2 O 4 Z -scheme with excellent visible-light photoactivity. <b>2023</b> , 106, 3594-3604	O
5	Boosting photocatalytic performances of lamellar BiVO4 by constructing S-scheme heterojunctions with AgBr for efficient charge transfer. <b>2023</b> , 34, 215703	O
4	Pressure-Optimized Band Gap and Enhanced Photoelectric Response of Graphitic Carbon Nitride with Nitrogen Vacancies. <b>2023</b> , 19,	О
3	A Review on Nano Ti-Based Oxides for Dark and Photocatalysis: From Photoinduced Processes to Bioimplant Applications. <b>2023</b> , 13, 982	O
2	Microwave Irradiation vs. Structural, Physicochemical, and Biological Features of Porous Environmentally Active SilverBilica Nanocomposites. <b>2023</b> , 24, 6632	Ο
1	Novel binary composite of manganese ferrite/tungsten disulfide as a superior photocatalyst and ultra-reusability in reduction of nitroarenes. <b>2023</b> , 178, 106671	О